NUREG/CR-4784
BNL-NUREG-52039

INFLUENCE OF GROUND WATER ON SOIL-STRUCTURE INTERACTION

C.J. Costantino and A.J. Philippacopoulos

Date Published — December 1987

DEPARTMENT OF NUCLEAR ENERGY, BROOKHAVEN NATIONAL LABORATORY
UPTON, NEW YORK 11973

Prepared for the U.S. Nuclear Regulatory Commission
Washington, D.C. 20555
Contract No. DE-AC02-76CH00016

NUREG/CR-4784
BNL-NUREG-52039
AN, RM

INFLUENCE OF GROUND WATER ON SOIL-STRUCTURE INTERACTION

C.J. Costantino and A.J. Philippacopoulos

THE CITY UNIVERSITY OF NEW YORK
Under Contract to the
STRUCTURAL ANALYSIS DIVISION
and
DEPARTMENT OF NUCLEAR ENERGY
BROOKHAVEN NATIONAL LABORATORY
UPTON, NEW YORK 11973

December 1987

Prepared for
OFFICE OF NUCLEAR REGULATORY RESEARCH
U.S. NUCLEAR REGULATORY COMMISSION
WASHINGTON, D.C. 20555
UNDER CONTRACT NO. DE-AC02-76CH00016
NRC FIN A3242

Available from
Superintendent of Documents
U.S. Government Printing Office
P.O. Box 37082
Washington, DC 20013-7982
and
National Technical Information Service
Springfield, Virginia 22161

ABSTRACT

This study has been performed for the Nuclear Regulatory Commission (NRC) by the Structural Analysis Division of Brookhaven National Laboratory (BNL). The study was conducted during the fiscal year 1986 on the program entitled "Benchmarking of Structural Engineering Problems" sponsored by NRC. The results presented herein were developed both at the City University of New York, under contract to BNL, as well as at BNL.

This report presents a summary of the second year's effort on the subject of the influence of foundation ground water on the SSI phenomenon. A finite element computer program, developed during the first year's effort, was used to study the impact of depth to the ground water surface on the SSI problem. The formulation used therein is based on the Biot dynamic equations of motion for both the solid and fluid phases of a typical soil. Frequency dependent interaction coefficients were then generated for the two-dimensional plane problem of a rigid surface footing moving against a linear soil. The soil is considered dry above the GWT and fully saturated below. The results indicate that interaction coefficients are significantly modified as compared to the comparable values for a dry soil, particularly for the rocking mode of response, if the GWT is close to the foundation. As the GWT moves away from the foundation, these effects decrease in a relatively orderly fashion for both the horizontal and rocking modes of response. For the vertical interaction coefficients, the rate of convergence to the dry solution is frequency dependent.

Calculations were made to study the impact of the modified interaction coefficients on the response of a typical nuclear reactor building. The amplification factors for a stick model placed atop a dry and saturated soil were computed. It was found that pore water caused the rocking response to decrease and translational response to increase over the frequency range of interest, as compared to the response on dry soil.

TABLE OF CONTENTS

LIST OF FIGURES

ACKNOWLEDGEMENTS

The authors wish to express their appreciation to Mr. Herman Graves for his advice and support during this program. Mr. Graves, of the Mechanical Structural Engineering Branch of the Office of Nuclear Regulatory Research, U.S. Nuclear Regulatory Commission, served as technical monitor of this study.

EXECUTIVE SUMMARY

This study has been performed for the Nuclear Regulatory Commission (NRC) by the Structural Analysis Division of Brookhaven National Laboratory (BNL). The study was conducted during the fiscal year 1986 on the program entitled "Benchmarking of Structural Engineering Problems" sponsored by NRC. The study was conducted in part at the City University of New York (CUNY) under subcontract to BNL.

This report presents a summary of the second year's effort on the subject of the influence of foundation ground water on the SSI phenomenon. During the first year's effort, a finite element computer program was developed for the two-phased formulation of the combined soil-water problem. This formulation is based on the Biot dynamic equations of motion for both the solid and fluid phases of a typical soil. Frequency dependent interaction coefficients were generated for the two-dimensional plane problem of a rigid surface footing moving against a saturated linear soil. The results indicated that interaction coefficients are significantly modified as compared to the comparable values for a dry soil, particularly for the rocking mode of response. Calculations were made to study the impact of the modified interaction coefficients on the response of a typical nuclear reactor building. It was found that pore water caused the rocking response to decrease and translational response to increase over the frequency range of interest, as compared to the response on dry soil.

For this year's effort, the computer program was modified to consider the foundation soil as dry above the ground water table (GWT). Again, frequency dependent interaction coefficients were generated, but in this case with the goal of attempting to determine the impact of the depth to the GWT on the computed responses. It should be pointed out that this effort did not include any effort to (a) increase the size or speed of the computer program developed previously, or (b) improve the transmitting boundary formulation in the saturated zone to improve computational accuracy.

The results found from these computations indicate that the computed interaction coefficients are significantly modified as compared to the comparable values for a fully dry foundation soil. This is particularly true for the rocking mode of response, when the GWT is close to the foundation level. If the pore water becomes essentially trapped within the soil skeleton due to

permeability, compressibility of the soil decreases, forcing the pore water to effectively carry a larger portion of the applied structural load. As the GWT moves further from the strucuture, these effects decrease in an orderly fashion for both the horizontal and rocking modes of response. For the vertical response mode, the rate of convergence to the dry solution is highly frequency dependent.

1.0 INTRODUCTION

This study has been conducted at the City University of New York (CUNY) under subcontract to Brookhaven National Laboratory (BNL). The work was sponsored by the Nuclear Regulatory Commission (NRC) on the "Benchmarking of Structural Engineering Problems" program, and was conducted during the fiscal year of 1986. This report represents a summary of the second year's effort on the subject of the influence of foundation ground water on the soil-structure interaction phenomena.

Soil-structure interaction has been, of course, a topic of major interest for many years in the area of geomechanics. The study of structural response to seismic inputs has been extensively investigated, and, particularly with the advent of the growth of digital computer capability, has lead to the development of numerical methods of analysis which are used as standard tools for the design of structures. One aspect of the soil-structure interaction process which has not been developed to the same degree of sophistication is the impact of ground water (or pore water) on the response of the soil-structure system. There are very good reasons for this state of affairs, however, not the least of which is the difficulty of incorporating this aspect into the analysis. One can consider that the impact of pore water effects is directly controlled by the magnitudes of the dynamic strains developed in the soil during the interaction process. At one extreme, at the large strain end of the spectrum, the engineer is concerned with the potential development of failure conditions under the structure, and is typically interested with the onset of liquefaction conditions in the soil. The current state of the art in this area is to a great extent based on empirical methods of analysis, generated from investigations of limited failure data from specific sites around the world. The difficulties encountered in this area stem primarily from a lack of knowledge of soil constitutive data at large strains.

At the small strain end of the spectrum, the analytic approaches that can be used to study the impact of pore water are more tenable, and in fact have a relatively long history, extending back some 40 odd years. To be sure, difficulties still exist in this area, and these again are primarily associated with constitutive properties of real soils. However, with the availability of

computer power, realistic problems can be investigated to at least allow engineers to assess the potential impact of pore water on seismic response. It is with this latter category that this study is concerned.

1.1 Objective and Scope of Study

As is well known, the various methods of seismic response analysis can be grouped into several distinct categories. In these various approaches, the structural models used can range from simple stick models composed of linear beam elements to complex finite element models. The key to the adequacy of the seismic analysis performed, however, is the adequacy of the developed interaction coefficients used to represent the influence of the soil foundation. For the one-phase, linear elastic material problem, various procedures are available with which to generate such coefficients. However, for the case of saturated soils, no such comparable capability is generally available to perform the soil-structure interaction analysis. In the first years' effort on this topic, a finite element computer program was generated to study the impact of pore water on the response. It is the goal of this study to generate estimates of the potential impact of ground water on the soil-structure interaction process.

The basic problem under consideration is shown in Figure 1.1, in which a linear flexible structure is situated at or near the surface of a soil half-space. In keeping with typical small strain seismic analyses, the soil skeleton is represented as a linear medium in which all potential nonlinearities are at most lumped together into an equivalent hysteretic damping modulus. The only additional fact included in this study is that the ground water level is located at some depth relatively close to the structure, and in a position to impact on the seismic response of the facility. In order to properly determine the response of this soil/water system, a two phased medium formulation was developed which treats the response of both the solids and water as two separate linear media which are coupled together through soil permeability effects. Such a formulation has been developed previously and is available for use in this study.

Since it is known that analytic solutions are available for only the simplest of configurations, a numerical finite element solution process was developed, as seen in Figure 1.2. Again, in keeping with typical SSI analyses, in

order to make the finite element approach yield reasonable results, a comparable transmitting boundary formulation was included in the original numerical development. The purpose of the transmitting boundary formulation is, of course, to allow for the treatment of extended soil/water halfspace problems. However, in the original study, a simple one dimensional transmitting boundary model was developed.

For this continuation of the program, a restricted effort was considered on the pore water problem, since other activities took precedence. The primary focus of this study was therefore limited to only two specific activities. The first objective was concerned with the development of information on the effect of depth to the ground water table on the interaction process. This phase of the study made use of the available computer program, written for the first years' effort, to generate interaction data as a function of ground water depth below the structure. A second activity was the beginning effort to improve the transmitting boundary formulation. To this end, the first half of the two dimensional transmitting boundary formulation was developed. This analytic formulation can then be used to complete the numerical development, if further activites are to be invested on the pore water problem.

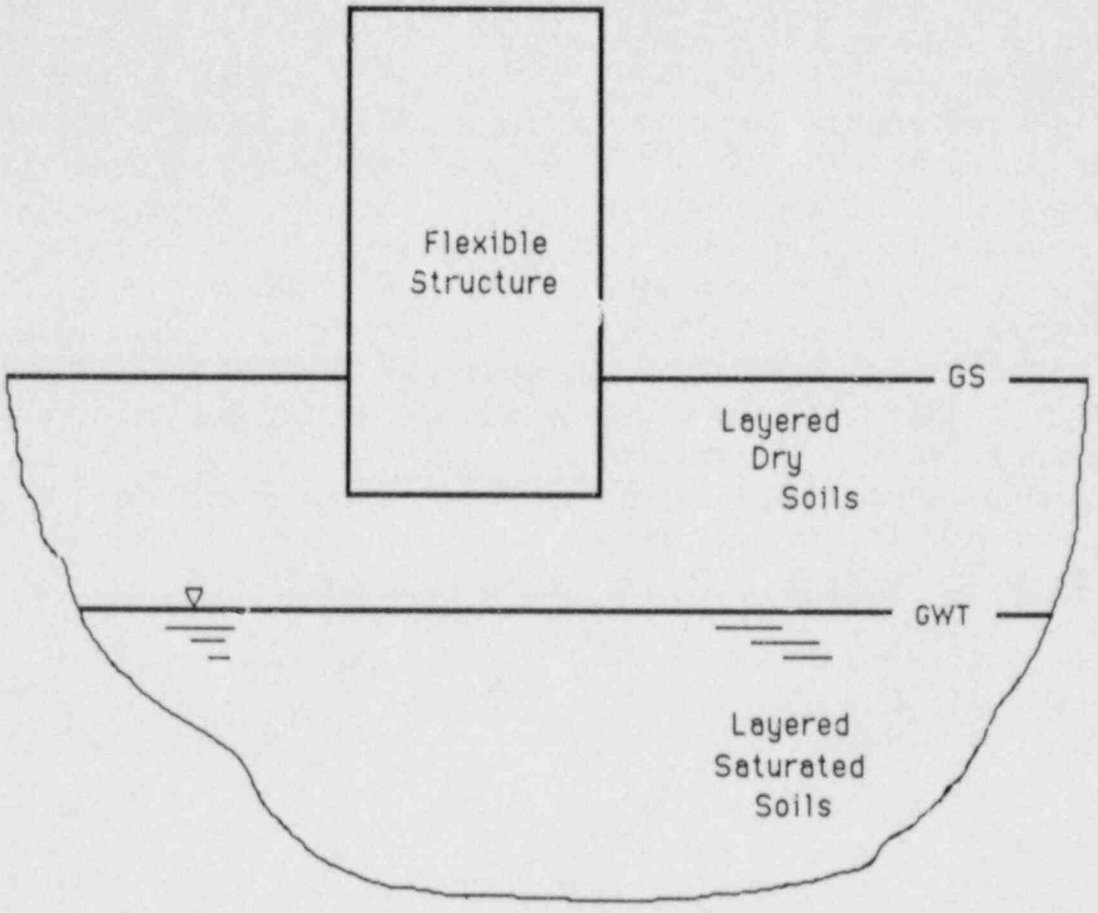

FIGURE 1.1 GENERALIZED PROBLEM DESCRIPTION

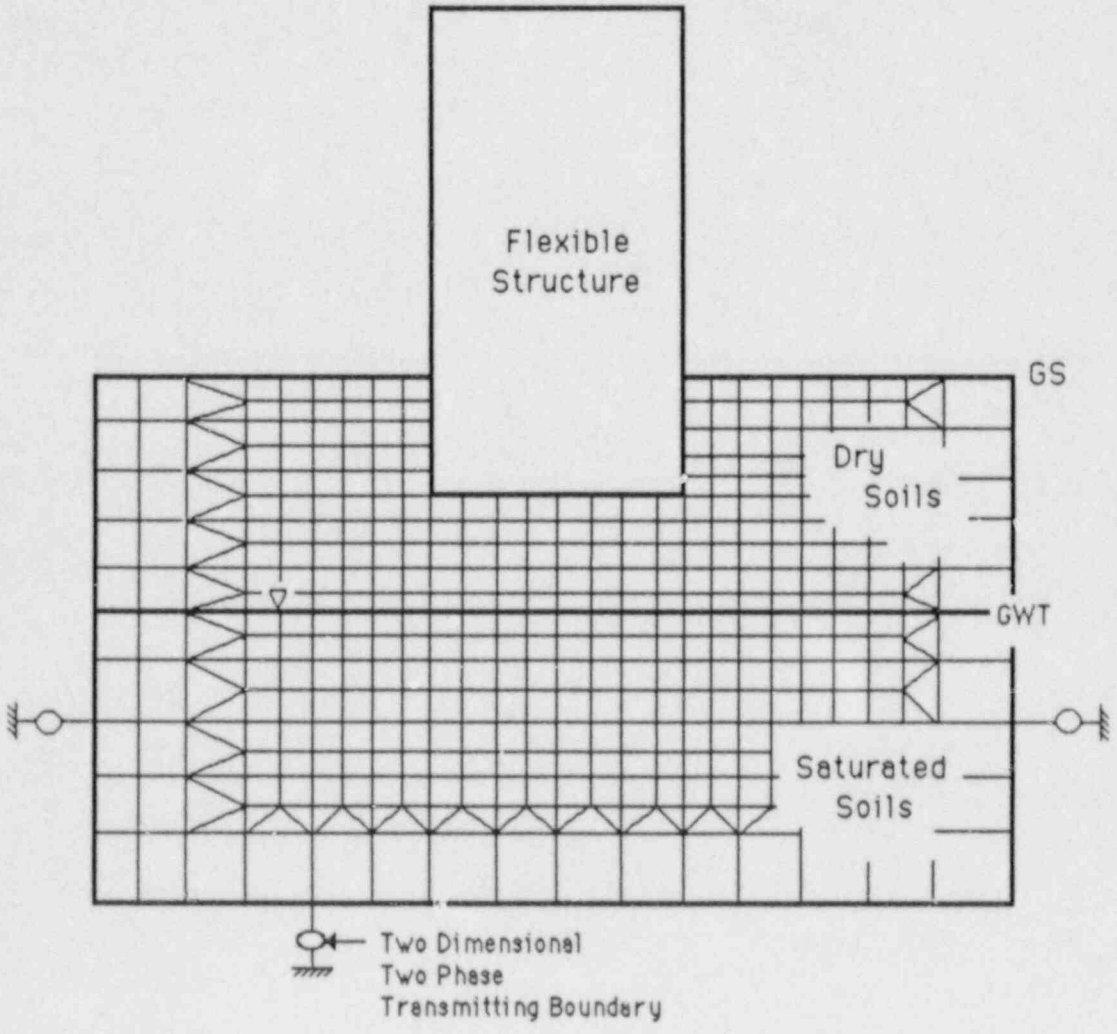

FIGURE 1.2 FINITE ELEMENT REPRESENTATION

2.0 GOVERNING SYSTEM EQUATIONS

The framework within which the governing system equations are developed is based upon the classical formulation of Biot (Ref. 5-11) for the general case of porous, linear elastic, two-phased media. This Biot model provides coupling between the solid and fluid stress states and includes the effects of fluid compressibility. Aside from the general three dimensional formulation, this latter effect is a significant deviation from the standard Terzaghi formulation that is typically used in standard approaches to consolidation studies. For completeness of this report, the Biot equations are presented in detail.

Denoting by (u_x, u_y, u_z) the components of displacement of the soil solids (soil skeketon), and using the standard assumptions of small strain, the strain-displacement relations can be written as:

$$\begin{aligned} \varepsilon_{xx} &= \frac{\partial u_x}{\partial x} & \varepsilon_{xy} &= \frac{\partial u_y}{\partial x} + \frac{\partial u_x}{\partial y} \\ \varepsilon_{yy} &= \frac{\partial u_y}{\partial y} & \varepsilon_{yz} &= \frac{\partial u_z}{\partial y} + \frac{\partial u_y}{\partial z} \\ \varepsilon_{zz} &= \frac{\partial u_z}{\partial z} & \varepsilon_{zx} &= \frac{\partial u_x}{\partial z} + \frac{\partial u_z}{\partial x} \end{aligned} \qquad (2.1)$$

Assuming the soil skeleton to possess isotropic elastic properties (included here for simplicity of the development), the corresponding stress-strain relations reduce to the simplified form as:

$$\begin{aligned} \varepsilon_{xx} &= \frac{1}{E}[\sigma_{xx} - \nu(\sigma_{yy} + \sigma_{zz})] & \varepsilon_{xy} &= \frac{\sigma_{xy}}{G} \\ \varepsilon_{yy} &= \frac{1}{E}[\sigma_{yy} - \nu(\sigma_{zz} + \sigma_{xx})] & \varepsilon_{yz} &= \frac{\sigma_{yz}}{G} \\ \varepsilon_{zz} &= \frac{1}{E}[\sigma_{zz} - \nu(\sigma_{xx} + \sigma_{yy})] & \varepsilon_{zx} &= \frac{\sigma_{zx}}{G} \end{aligned} \qquad (2.2)$$

In the above equations, the coefficients E, G and ν are Young's modulus, shear modulus and Poisson's ratio of the soil skeleton. The stresses (σ_{xx} .. σ_{yz}) are the stresses sustained by the solid skeleton (the so-called intergranular or

effective soil stresses). Of course, the shear modulus is related to the other two elastic coefficients by

$$G = \frac{E}{2(1+\nu)} \tag{2.3}$$

Equations 2.2 can be simply inverted to yield

$$\{\sigma\} = [D]\{e\} \tag{2.4}$$

where

$$\begin{aligned} \{\sigma\} &= \{\sigma_{xx}, \sigma_{yy}, \sigma_{zz}, \sigma_{xy}, \sigma_{yz}, \sigma_{zx}\} \\ \{e\} &= \{e_{xx}, e_{yy}, e_{zz}, e_{xy}, e_{yz}, e_{zx}\} \end{aligned} \tag{2.5}$$

and

$$[D] = \begin{bmatrix} 1 & a & a & 0 & 0 & 0 \\ a & 1 & a & 0 & 0 & 0 \\ a & a & 1 & 0 & 0 & 0 \\ 0 & 0 & 0 & b & 0 & 0 \\ 0 & 0 & 0 & 0 & b & 0 \\ 0 & 0 & 0 & 0 & 0 & b \end{bmatrix} \tag{2.6}$$

$$E_c = \frac{(1-\nu)E}{(1+\nu)(1-2\nu)}$$

$$a = \frac{\nu}{(1-\nu)}, \qquad b = \frac{(1-2\nu)}{2(1-\nu)}$$

When the effects of pore pressure are included, the bulk (or total) stresses must also be considered. The components of the total stress tensor are denoted herein as τ_{ij}, where i,j = x,y or z. Considering a unit volume of bulk material (solid plus fluid), we denote the components of the fluid displacement vector as (U_x, Uy, Uz). These components are defined such that the volumes of fluid displaced through unit areas in the x,y and z directions are fU_x, fU_y, and fU_z respectively, where f

denotes the porosity of the solid skeleton. The flow of the fluid relative to the solid skeleton, but measured in terms of the volume per unit area of the bulk medium is

$$\begin{aligned} w_x &= f(U_x - u_x) \\ w_y &= f(U_y - u_y) \\ w_z &= f(U_z - u_z) \end{aligned} \tag{2.7}$$

The fluid volumetric strain is obtained by Biot as

$$\psi = -\left(\frac{\partial w_x}{\partial x} + \frac{\partial w_y}{\partial y} + \frac{\partial w_z}{\partial z}\right) \tag{2.8}$$

He has shown that the pore pressure can be written in terms of the volume change of the solid fraction as well as the compressibility of both the fluid and solid fractions by

$$p_f = -\alpha M(e_{xx} + e_{yy} + e_{zz}) + M\psi \tag{2.9}$$

where α is defined as the compressibility of the solid fraction and M is the compressibility of the fluid fraction. The bulk (or total) stress tensor is then given by

$$\begin{aligned} \tau_{xx} &= \sigma_{xx} - \alpha p_f & \tau_{xy} &= \sigma_{xy} \\ \tau_{yy} &= \sigma_{yy} - \alpha p_f & \tau_{yz} &= \sigma_{yz} \\ \tau_{zz} &= \sigma_{zz} - \alpha p_f & \tau_{zx} &= \sigma_{zx} \end{aligned} \tag{2.10}$$

Substituting 2.9 into 2.10 and using 2.4 yields the following bulk stress relations

$$\{\tau\} = ([D] + \alpha^2 M[D^*])\{e\} + \alpha M[\delta]\{w\} \tag{2.11}$$

where

$$\{\tau\} = \{\tau_{xx}, \tau_{yy}, \tau_{zz}, \tau_{xy}, \tau_{yz}, \tau_{zx}\} \tag{2.12}$$

$$\{w\} = \{w_x, w_y, w_z\}$$

and

$$[D^*] = \begin{bmatrix} 1 & 1 & 1 & 0 & 0 & 0 \\ 1 & 1 & 1 & 0 & 0 & 0 \\ 1 & 1 & 1 & 0 & 0 & 0 \\ 0 & 0 & 0 & 0 & 0 & 0 \\ 0 & 0 & 0 & 0 & 0 & 0 \\ 0 & 0 & 0 & 0 & 0 & 0 \end{bmatrix} \tag{2.13}$$

$$[\delta] = \begin{bmatrix} \partial/\partial x & \partial/\partial y & \partial/\partial z \\ \partial/\partial x & \partial/\partial y & \partial/\partial z \\ \partial/\partial x & \partial/\partial y & \partial/\partial z \\ 0 & 0 & 0 \\ 0 & 0 & 0 \\ 0 & 0 & 0 \end{bmatrix}$$

The kinetic energy per unit bulk volume is determined from

$$\begin{aligned} T = {} & \left(\frac{\rho}{2}\right)(\dot{u}_x^2 + \dot{u}_y^2 + \dot{u}_z^2) + \\ & (\rho_f)(\dot{u}_x\dot{w}_x + \dot{u}_y\dot{w}_y + \dot{u}_z\dot{w}_z) + \\ & \left(\frac{m}{2}\right)(\dot{w}_x^2 + \dot{w}_y^2 + \dot{w}_z^2) \end{aligned} \tag{2.14}$$

where

$$m = \frac{\rho_f}{f}$$

f = porosity
ρ = total mass density of bulk material
ρ_f = fluid mass density

The energy dissipation per unit bulk volume is given by Biot as

$$D = \left(\frac{\eta}{2k}\right)(\dot{w}_x^2 + \dot{w}_y^2 + \dot{w}_z^2) \tag{2.15}$$

where

η = fluid viscosity
k = soil permeability

We can now apply Lagrange's equations to this system, considering (u_x, u_y, u_z) and (w_x, w_y, w_z) as the generalized coordinates to develop the equations of motion. Considering first the displacements u_i, Lagrange's equations are

$$\frac{d}{dt}\left(\frac{\partial T}{\partial \dot{u}_i}\right) - \frac{\partial T}{\partial u_i} = Q_i \qquad (2.16)$$

If we define x and y as the horizontal coordinate directions and z as the vertical coordinate direction (positive down), we obtain the specific equations of motion as

$$\frac{d}{dt}\left(\frac{\partial T}{\partial \dot{u}_x}\right) = \rho \ddot{u}_x + \rho_f \ddot{w}_x$$

$$\frac{\partial T}{\partial u_x} = 0$$

$$Q_x = \frac{\partial \tau_{xx}}{\partial x} + \frac{\partial \tau_{xy}}{\partial y} + \frac{\partial \tau_{xz}}{\partial z} + \rho g_x$$

etc. But $g_x = g_y = 0$. Therefore the equations of motion can be written as

$$\begin{aligned}
\frac{\partial \tau_{xx}}{\partial x} + \frac{\partial \tau_{xy}}{\partial y} + \frac{\partial \tau_{xz}}{\partial z} &= \rho \ddot{u}_x + \rho_f \ddot{w}_x \\
\frac{\partial \tau_{yx}}{\partial x} + \frac{\partial \tau_{yy}}{\partial y} + \frac{\partial \tau_{yz}}{\partial z} &= \rho \ddot{u}_y + \rho_f \ddot{w}_y \qquad (2.17) \\
\frac{\partial \tau_{zx}}{\partial x} + \frac{\partial \tau_{zy}}{\partial y} + \frac{\partial \tau_{zz}}{\partial z} + \rho g_z &= \rho \ddot{u}_z + \rho_f \ddot{w}_z
\end{aligned}$$

Similarly, considering the coordinates w_i, where i = x, y, or z, Lagrange's equations are

$$\frac{d}{dt}\left(\frac{\partial T}{\partial \dot{w}_i}\right) + \frac{\partial D}{\partial \dot{w}_i} = -\frac{\partial p_f}{\partial t} + \rho_f g_i \qquad (2.18)$$

Therefore

$$
\begin{aligned}
-\frac{\partial p_f}{\partial x} &= \rho_f \ddot{u}_x + \frac{\rho_f}{f}\ddot{w}_x + \frac{\eta}{k}\dot{w}_x \\
-\frac{\partial p_f}{\partial y} &= \rho_f \ddot{u}_y + \frac{\rho_f}{f}\ddot{w}_y + \frac{\eta}{k}\dot{w}_y \\
-\frac{\partial p_f}{\partial z} &= \rho_f \ddot{u}_z + \frac{\rho_f}{f}\ddot{w}_z + \frac{\eta}{k}\dot{w}_z - \rho_f g_z
\end{aligned}
\qquad (2.19)
$$

Equations 2.17 and 2.19 represent the governing equations at a point in the two-phased solid/fluid medium. For the special case of a two-dimensional plane strain condition, these equations can easily be reduced to yield the following.

$$
\begin{aligned}
\frac{\partial \tau_{xx}}{\partial x} + \frac{\partial \tau_{xy}}{\partial y} &= \rho \ddot{u}_x + \rho_f \ddot{w}_x \\
\frac{\partial \tau_{yx}}{\partial x} + \frac{\partial \tau_{yy}}{\partial y} &= \rho \ddot{u}_y + \rho_f \ddot{w}_y
\end{aligned}
\qquad (2.20)
$$

while equations 2.19 become

$$
\begin{aligned}
-\frac{\partial p_f}{\partial x} &= \rho_f \ddot{u}_x + \frac{\rho_f}{f}\ddot{w}_x + \frac{\eta}{k}\dot{w}_x \\
-\frac{\partial p_f}{\partial y} &= \rho_f \ddot{u}_y + \frac{\rho_f}{f}\ddot{w}_y + \frac{\eta}{k}\dot{w}_y
\end{aligned}
\qquad (2.21)
$$

For the linear problem of interest herein, the gravitational force (or body force) can be removed since its effect can be obtained by simple superposition of a static solution to the dynamic stress state. All displacements and stresses presented are therefore values in excess of the static solution.

For the two-dimensional plane strain condition, the strain-displacement relations are

$$\{e\} = \begin{Bmatrix} e_{xx} \\ e_{yy} \\ e_{xy} \end{Bmatrix} = \begin{Bmatrix} \partial u_x/\partial x \\ \partial u_y/\partial y \\ \partial u_y/\partial x + \partial u_x/\partial y \end{Bmatrix} \tag{2.22}$$

The corresponding stress-strain relations are

$$\{\sigma\} = \begin{Bmatrix} \sigma_{xx} \\ \sigma_{yy} \\ \sigma_{xy} \end{Bmatrix} = E_c \begin{bmatrix} 1 & a & 0 \\ a & 1 & 0 \\ 0 & 0 & b \end{bmatrix} \tag{2.23}$$

where E_c, the confined modulus, and a and b are as were defined previously in (2.6). From equation 2.9, the pore pressure can be determined from

$$p_f = - \alpha M(e_{xx}+e_{yy}) + M\psi \tag{2.24}$$

where

$$\psi = - \left(\frac{\partial w_x}{\partial x} + \frac{\partial w_y}{\partial y}\right) \tag{2.25}$$

In matrix form, equation 2.24 becomes

$$p_f = - \alpha M \begin{Bmatrix} \partial/\partial x \\ \partial/\partial y \end{Bmatrix}^T \begin{Bmatrix} u_x \\ u_y \end{Bmatrix} - M \begin{Bmatrix} \partial/\partial x \\ \partial/\partial y \end{Bmatrix}^T \begin{Bmatrix} w_x \\ w_y \end{Bmatrix} \tag{2.26}$$

The bulk stress tensor is then

$$\{\tau\} = \begin{Bmatrix} \tau_{xx} \\ \tau_{yy} \\ \tau_{xy} \end{Bmatrix} = \begin{Bmatrix} \sigma_{xx} - \alpha p_f \\ \sigma_{yy} - \alpha p_f \\ \sigma_{xy} \end{Bmatrix} \tag{2.27}$$

Combining equations 2.22, 2.23 and 2.24 leads to

$$\{\tau\} = (E_c[D_0][D_1] + \alpha^2 M[D_2]) \begin{Bmatrix} u_x \\ u_y \end{Bmatrix} + \alpha M[D_2] \begin{Bmatrix} w_x \\ w_y \end{Bmatrix} \tag{2.28}$$

where

$$[D_o] = \begin{bmatrix} 1 & a & 0 \\ a & 1 & 0 \\ 0 & 0 & b \end{bmatrix}$$

$$[D_1] = \begin{bmatrix} \partial/\partial x & 0 \\ 0 & \partial/\partial y \\ \partial/\partial y & \partial/\partial x \end{bmatrix} \qquad (2.29)$$

$$[D_2] = \begin{bmatrix} \partial/\partial x & \partial/\partial y \\ \partial/\partial x & \partial/\partial y \\ 0 & 0 \end{bmatrix}$$

and a and b are as previously defined. If hysteretic damping effects are to be included in the problem (as is typically the case in the one-phase soil-structure interaction analysis), equation 2.28 can be modified to

$$\{\tau\} = E_c[D_o][D_1]\begin{Bmatrix} u_x \\ u_y \end{Bmatrix} + E_c[D_3][D_1]\begin{Bmatrix} \partial u_x/\partial t \\ \partial u_y/\partial t \end{Bmatrix} + \alpha^2 M[D_2]\begin{Bmatrix} u_x \\ u_y \end{Bmatrix} + \alpha M[D_2]\begin{Bmatrix} w_x \\ w_y \end{Bmatrix} \qquad (2.30)$$

where

$$[D_3] = \begin{bmatrix} \lambda_c & \lambda_c a & 0 \\ \lambda_c a & \lambda_c & 0 \\ 0 & 0 & \lambda_s b \end{bmatrix} \qquad (2.31)$$

In equation 2.31, the term λ_c represents the hysteretic damping ratio associated with hydrostatic compression while λ_s represents the hysteretic damping ratio associated with deviatoric (or shear) strains. It should be pointed out that although separate damping ratios for the hydrostatic and shearing stress states are not usually used in SSI analyses, it is more probable that for typical soils these two ratios should in fact be different. The primary purpose for including this capability at this stage of the study is to improve the capability of the developed computer program. Numerical results will be generated at a later time

to ascertain the impact of this effect.

Considering steady state solutions for this linear problem, we will use the general notation (unless otherwise indicated) of a super-bar to indicate the complex amplitude of a parameter. Thus, we use the form

$$\{u\} = \{\bar{u}\}e^{i\Omega t}, \quad \{w\} = \{\bar{w}\}e^{i\Omega t}, \quad \text{etc.} \tag{2.32}$$

and at the same time define the parameters $\theta = \Omega x/U_c$ and $\Phi = \Omega y/U_c$ as the dimensionless space coordinates. In addition, the following parameters are also defined:

$$U_c = \sqrt{\frac{E_c + \alpha^2 M}{\rho}}$$

$$N = \frac{\rho_f}{f} \tag{2.33}$$

$$K = \frac{M}{E_c + \alpha^2 M}$$

With the aid of equations 2.32 and 2.33, equation 2.26 becomes

$$\bar{p}_f = -\frac{\alpha M\Omega}{U_c}\left\{\begin{matrix}\partial/\partial\theta \\ \partial/\partial\Phi\end{matrix}\right\}^T\left\{\begin{matrix}\bar{u}_x \\ \bar{u}_y\end{matrix}\right\} - \frac{M\Omega}{U_c}\left\{\begin{matrix}\partial/\partial\theta \\ \partial/\partial\Phi\end{matrix}\right\}^T\left\{\begin{matrix}\bar{w}_x \\ \bar{w}_y\end{matrix}\right\} \tag{2.34}$$

Equations 2.30 become

$$\{\bar{\tau}\} = \left(\frac{E_c\Omega}{U_c}\right)[D_0][D_4]\{\bar{u}\} + i\left(\frac{E_c\Omega^2}{U_c}\right)[D_3][D_4]\{\bar{u}\} + \left(\frac{\alpha^2 M\Omega}{U_c}\right)[D_5]\{\bar{u}\} + \left(\frac{\alpha M\Omega}{U_c}\right)[D_5]\{\bar{w}\} \tag{2.35}$$

where

$$[D_4] = \begin{bmatrix} \partial/\partial\theta & 0 \\ 0 & \partial/\partial\phi \\ \partial/\partial\phi & \partial/\partial\theta \end{bmatrix} \tag{2.36}$$

$$[D_5] = \begin{bmatrix} 1 & 1 & 0 \\ 1 & 1 & 0 \\ 0 & 0 & 0 \end{bmatrix} [D_4] \tag{2.37}$$

With the aid of equation 2.35, equations 2.20 can be written in matrix form as

$$\begin{aligned} &[D_4] \left\{ \left(\frac{E_c}{\rho U_c^2} \right) [D_0][D_4]\{\bar{u}\} \right. \\ &+ i \left(\frac{\Omega E_c}{\rho U_c^2} \right) [D_3][D_4]\{\bar{u}\} + (\alpha^2 K)[D_5]\{\bar{u}\} \\ &\left. + (\alpha K)[D_5]\{\bar{w}\} \right\} + \{\bar{u}\} + N\{\bar{w}\} = 0 \end{aligned} \tag{2.38}$$

Similarly, with the aid of equation 2.34, equations 2.21 can be written in matrix form as

$$\begin{aligned} &\left\{ \begin{matrix} \partial/\partial\theta \\ \partial/\partial\phi \end{matrix} \right\} \left\{ \begin{matrix} \partial/\partial\theta \\ \partial/\partial\phi \end{matrix} \right\}^T \left\langle (\alpha K)\{\bar{u}\} + K\{\bar{w}\} \right\rangle \\ &+ N\{\bar{u}\} + \left(\frac{N}{f} \right)\{\bar{w}\} - i \left(\frac{\eta}{\rho k \Omega} \right)\{\bar{w}\} = 0 \end{aligned} \tag{2.39}$$

3.0 FREE WAVE SOLUTION

As stated previously, the principal focus of this study has been the attempt to determine the effects of ground water as a function of depth to the ground water table, with the overall goal being to estimate when ground water effects are negligible. Numerical finite element solutions will be presented for this problem in the next section, but as would generally be anticipated, the numerical results will be limited to the particular configuration analyzed. In an attempt to generated a more general result, an analytic solution is presented for the free wave solution to the wave propagation problem. This solution has the added advantage of being available for the development of an improved transmitting boundary formulation at a later date.

The specific configuration considered is shown in Figure 3.1 and consists of the two dimensional plane strain elastic halfspace with the ground water table (GWT) located at a depth H below the ground surface (GS). We now proceed to develop solutions in each zone, with the goal of matching solutions by the interface conditions at the depth H.

3.1 General Solution For Saturated Soil

For the saturated zone of this halfspace, the equilibrium equations are given by equations 2.20 and 2.21, with the corresponding stress-displacement relations presented in equations 2.26 and 2.27. These equations are combined to yield

$$
\begin{aligned}
G(u_{x,xx} + u_{x,yy}) + (G+\lambda^*)e_{,x} - \alpha M\zeta_{,x} &= \rho\ddot{u}_x + \rho_f\ddot{w}_x \\
G(u_{y,xx} + u_{y,yy}) + (G+\lambda^*)e_{,y} - \alpha M\zeta_{,y} &= \rho\ddot{u}_y + \rho_f\ddot{w}_y \\
(\alpha Me - M\zeta)_{,x} &= \rho_f\ddot{u}_x + m\ddot{w}_x + (\eta/k)\dot{w}_x \\
(\alpha Me - M\zeta)_{,y} &= \rho_f\ddot{u}_y + m\ddot{w}_y + (\eta/k)\dot{w}_y
\end{aligned}
\qquad (3.1)
$$

where $e = (u_{x,x} + u_{y,y})$

$$\zeta = -(w_{x,x} + w_{y,y}) \tag{3.2}$$

and

$$m = \rho_f / f \qquad \lambda^* = \lambda + \alpha^2 M$$

$$\lambda = \left[\frac{\nu}{1-\nu}\right] E_c, \quad E_c = E\left[\frac{1-\nu}{(1+\nu)(1-2\nu)}\right]$$

Potential functions (Φ_2, Φ_3) and (Ψ_2, Ψ_3) are defined in the usual way such that the displacement components are expressed as

$$u_x = \Phi_{2,x} - \Psi_{2,y} \qquad w_x = \Phi_{3,x} - \Psi_{3,y}$$

$$u_y = \Phi_{2,y} + \Psi_{2,x} \qquad w_y = \Phi_{3,y} + \Psi_{3,x} \tag{3.3}$$

and

$$e = (\Phi_{2,xx} + \Phi_{2,yy}) \qquad \zeta = -(\Phi_{3,xx} + \Phi_{3,yy}) \tag{3.4}$$

Substituting 3.3 and 3.4 into 3.1 leads after some manipulation to

$$(\lambda^*+2G)\nabla^2\Phi_2 + \alpha M\nabla^2\Phi_3 = \rho\Phi_{2,tt} + \rho_f \Phi_{3,tt}$$

$$G\nabla^2\Psi_2 = \rho \Psi_{2,tt} + \rho_f \Psi_{3,tt} \tag{3.5}$$

and

$$\alpha M\nabla^2\Phi_2 + M\nabla^2\Phi_3 = \rho_f\Phi_{2,tt} + m\Phi_{3,tt} + (\eta/k)\Phi_{3,t}$$

$$\rho_f\Psi_{2,tt} + m\Psi_{3,tt} + (\eta/k) = 0 \tag{3.6}$$

For the purposes of convenience, equations 3.5 and 3.6 can be written in matrix form as

$$\nabla^2\begin{bmatrix}(\lambda^*+2G) & \alpha M\\ \alpha M & M\end{bmatrix}\begin{Bmatrix}\Phi_2\\ \Phi_3\end{Bmatrix} =$$

$$\begin{bmatrix}\rho & \rho_f\\ \rho_f & m\end{bmatrix}\begin{Bmatrix}\Phi_2\\ \Phi_3\end{Bmatrix}_{,tt} + \begin{bmatrix}0 & 0\\ 0 & (\eta/k)\end{bmatrix}\begin{Bmatrix}\Phi_2\\ \Phi_3\end{Bmatrix}_{,t} \qquad (3.7)$$

and

$$\nabla^2\begin{bmatrix}G & 0\\ 0 & 0\end{bmatrix}\begin{Bmatrix}\Psi_2\\ \Psi_3\end{Bmatrix} =$$

$$\begin{bmatrix}\rho & \rho_f\\ \rho_f & m\end{bmatrix}\begin{Bmatrix}\Psi_2\\ \Psi_3\end{Bmatrix}_{,tt} + \begin{bmatrix}0 & 0\\ 0 & (\eta/k)\end{bmatrix}\begin{Bmatrix}\Psi_2\\ \Psi_3\end{Bmatrix}_{,t} \qquad (3.8)$$

Equations 3.7 and 3.8 are the wave equations for the dilatational and distortional propagation in the fully saturated soil system. It is easily shown that these waves are uncoupled.

Assuming now a plane wave traveling in the x-direction, the potential functions (Φ_2, Φ_3) admit the solution in the exponential form

$$\begin{Bmatrix}\Phi_2\\ \Phi_3\end{Bmatrix} = \begin{Bmatrix}\bar{\Phi}_2\\ \bar{\Phi}_3\end{Bmatrix} e^{[i(\omega t - px) + \xi y]} \qquad (3.9)$$

By substituting equation 3.9 into 3.7 leads to

$$\begin{bmatrix}\{-(\lambda^*+2G)\Lambda^2+\rho\omega^2\} & \{-\alpha M\Lambda^2+\rho_f\omega^2\}\\ \{-\alpha M\Lambda^2+\rho_f\omega^2\} & \{-M\Lambda^2+m\omega^2-i\left(\frac{\eta\omega}{k}\right)\}\end{bmatrix}\begin{Bmatrix}\bar{\Phi}_2\\ \bar{\Phi}_3\end{Bmatrix} = 0 \qquad (3.10)$$

where Λ^2 is defined as

$$\Lambda^2 = (p^2-\xi^2) \qquad (3.11)$$

The nontrivial solution for (Φ_2, Φ_3) requires that the determinant of 3.10 vanish, leading to the following relation

$$[M(\lambda+2G)]\left(\frac{\Lambda}{\omega}\right)^4$$

$$+\{2\alpha M\rho_f - \rho M - (\lambda^*+2G)[m-i\left(\frac{\eta}{k}\right)]\}\left(\frac{\Lambda}{\omega}\right)^2 \qquad (3.12)$$

$$+[\rho m - \rho_f^2 - i\left(\frac{\rho\eta}{k\omega}\right)] = 0$$

The solution to 3.12 leads to

$$\left(\frac{\Lambda}{\omega}\right)^2_{1,2} = A \pm B \qquad (3.13)$$

where

$$A = -\frac{1}{2M(\lambda+2G)}\{(2\alpha\rho_f-\rho) - (\lambda^*+2G)(m-i\frac{\eta}{k\omega})\}$$

$$B = \frac{1}{2M(\lambda+2G)}\{\beta_1 + i\beta_2\}^{1/2}$$

and

$$\beta_1 = \left[(2\alpha\rho_f-\rho)M - (\lambda^*+2G)m\right]^2$$

$$- \left[(\lambda^*+2G)\left(\frac{\eta}{k\omega}\right)\right]^2 - \left[4M(\lambda+2G)(\rho m-\rho_f^2)\right]$$

$$\beta_2 = \left(\frac{2\eta}{k\omega}\right)\left[\{(2\alpha\rho_f-\rho)M - (\lambda^*+2G)m\}(\lambda^*+2G) + 2\rho M(\lambda+2G)\right]$$

From equation 3.11, the eigensolution for ξ is then given by

$$\xi_{1,2} = p\left[1 - \left(\frac{\omega}{p\bar{\alpha}_{1,2}}\right)^2\right]^{1/2} \tag{3.14}$$

where

$$\bar{\alpha}_{1,2} = \frac{\omega}{\Lambda_{1,2}} \tag{3.15}$$

Substituting this eigensolution into equation 3.10 leads to the "shape functions"

$$\Phi_2 = \Phi_3\, \delta_{1,2} \tag{3.16}$$

where

$$\delta_{1,2} = \frac{\left[\alpha M \left(\frac{\Lambda}{\omega}\right)^2_{1,2} - \rho_f\right]}{\left[\rho - (\lambda^* + 2G)\left(\frac{\Lambda}{\omega}\right)^2_{1,2}\right]}$$

In a similar fashion, solutions for the distortional wave can be obtained by assuming a solution in the form

$$\begin{Bmatrix} \Psi_2 \\ \Psi_3 \end{Bmatrix} = \begin{Bmatrix} \Psi_2 \\ \Psi_3 \end{Bmatrix} e^{[i(\omega t - px) + \xi y]} \tag{3.17}$$

Substituting 3.17 into equation 3.8 yields the matrix equation

$$\begin{bmatrix} [-G\Gamma^2 + \rho\omega^2] & \rho_f\omega^2 \\ \rho_f\omega^2 & [m\omega^2 - i\left(\frac{\eta\omega}{k}\right)] \end{bmatrix} \begin{Bmatrix} \Psi_2 \\ \Psi_3 \end{Bmatrix} = 0 \tag{3.18}$$

where Γ is defined as

$$\Gamma^2 = (\rho^2 - \xi^2) \tag{3.19}$$

The eigen equation leading to a nontrivial solution is

$$\left(\frac{\Gamma}{\omega}\right)^2 = \frac{\left[\rho_f^2 - m\rho + i\rho\left(\frac{\eta}{k\omega}\right)\right]}{G\left[-m + i\left(\frac{\eta}{k\omega}\right)\right]} \tag{3.20}$$

and the corresponding eigen vector given by

$$\Psi_3 = \delta_3 \Psi_2 \tag{3.21}$$

where

$$\delta_3 = -\frac{\left[-G\left(\frac{\Gamma}{\omega}\right)^2 + \rho\right]}{\rho_f} \tag{3.22}$$

and from the definition of equation 3.19

$$\xi_3 = p\left[1 - \left(\frac{\omega}{p\bar{\beta}}\right)^2\right] \tag{3.23}$$

where

$$\bar{\beta} = \left(\frac{\omega}{\Gamma}\right) \tag{3.24}$$

Thus the potential solutions for this free wave problem in the saturated zone can be written as

$$\Phi_2 = [\ A_1 e^{\xi_1 y} + A_2 e^{\xi_2 y}]\ e^{[i(\omega t - px)]}$$
$$\Phi_3 = [\delta_1 A_1 e^{\xi_1 y} + \delta_2 A_2 e^{\xi_2 y}]\ e^{[i(\omega t - px)]} \qquad (3.25)$$
$$\Psi_2 = [\ B e^{\xi_3 y}\ ]\ e^{[i(\omega t - px)]}$$
$$\Psi_3 = [\delta_3 B e^{\xi_3 y}\ ]\ e^{[i(\omega t - px)]}$$

Substituting these solutions into the potential definitions of equations 3.3 and the stress-displacement relations of equations 2.26 and 2.28 leads to the following relations:

$$u_x = -\left[e^{i(\omega t - px)}\right]\left[ip\left(A_1 e^{\xi_1 y} + A_2 e^{\xi_2 y}\right) + \xi_3 B e^{\xi_3 y}\right]$$
$$u_y = \left[e^{i(\omega t - px)}\right]\left[\left(\xi_1 A_1 e^{\xi_1 y} + \xi_2 A_2 e^{\xi_2 y}\right) - ipB e^{\xi_3 y}\right] \qquad (3.26)$$
$$w_x = -\left[e^{i(\omega t - px)}\right]\left[ip\left(\delta_1 A_1 e^{\xi_1 y} + \delta_2 A_2 e^{\xi_2 y}\right) + \delta_3 \xi_3 B e^{\xi_3 y}\right]$$
$$w_y = \left[e^{i(\omega t - px)}\right]\left[\left(\delta_1 \xi_1 A_1 e^{\xi_1 y} + \delta_2 \xi_2 A_2 e^{\xi_2 y}\right) - ip\delta_3 B e^{\xi_3 y}\right]$$

and

$$\tau_{xx} = e^{[i(\omega t - px)]}\{-[2Gp^2 + (\lambda^* + \alpha M \delta_1)\Lambda_1^2]A_1 e^{(\xi_1 y)} - [2Gp^2 + (\lambda^* + \alpha M \delta_2)\Lambda_2^2]A_2 e^{(\xi_2 y)} + i[2Gp\xi_3]B e^{(\xi_3 y)}\}$$

$$\tau_{yy} = e^{[i(\omega t-px)]}\{[2Gp^2-(2G+\lambda^*+\alpha M\delta_1)\Lambda_1^2]A_1e^{(\xi_1 y)} +[2Gp^2-(2G+\lambda^*+\alpha M\delta_2)\Lambda_2^2]A_2e^{(\xi_2 y)} -i[2Gp\xi_3]Be^{(\xi_3 y)}\}$$

(3.27)

$$\tau_{xy} = e^{[i(\omega t-px)]}\{-[i2Gp\xi_1]A_1e^{(\xi_1 y)} - [i2Gp\xi_2]A_2e^{(\xi_2 y)} -[p^2+\xi^2]Be^{(\xi_3 y)}\}$$

$$p_f = e^{[i(\omega t-px)]}\{[(\alpha_1+\delta_1)\Lambda_1^2]A_1e^{(\xi_1 y)} +[(\alpha+\delta_2)\Lambda_2^2]A_2e^{(\xi_2 y)}\}$$

3.2 General Solution for Dry Soil

A similar solution can be generated for the case of a dry, single-phased soil, which would apply for the upper soil zone. The solution can be obtained for the saturated solution by setting M, ρ_f and η equal to zero. The equations of motion are

$$G(u_{x,xx} + u_{x,yy}) + (\lambda+G)(u_{x,xx} + u_{y,xy}) = \rho\, u_{x,tt}$$
$$G(u_{y,xx} + u_{y,yy}) + (\lambda+G)(u_{x,xy} + u_{y,yy}) = \rho\, u_{y,tt} \qquad (3.28)$$

Assuming again potential functions ϕ_1 and ψ_1 defined as

$$u_x = \phi_{1,x} - \psi_{1,y} \qquad \text{and} \qquad u_y = \phi_{1,y} + \psi_{1,x} \qquad (3.29)$$

equations 3.28 reduce to uncoupled wave equations for the compressional and distortional modes of motion as

$$\alpha_L^2 \nabla^2 \Phi_1 = \Phi_{1,tt}$$
$$\beta_L^2 \nabla^2 \Psi_1 = \Psi_{1,tt} \qquad (3.30)$$

where

$$\alpha_L^2 = \frac{\lambda + 2G}{\rho}, \qquad \beta_L^2 = \frac{G}{\rho}$$

In a similar fashion, equations 3.30 admit solutions of the form

$$\begin{Bmatrix} \Phi_1 \\ \Psi_1 \end{Bmatrix} = \begin{Bmatrix} \bar{\Phi}_1 \\ \bar{\Psi}_1 \end{Bmatrix} e^{[i(\omega t - px) + qz]}$$

The solutions to equations 3.30 can then be written as

$$\bar{\Phi}_1 = A_3 e^{-qy} + A_4 e^{qy}$$
$$\bar{\Psi}_1 = B_1 e^{-qy} + B_2 e^{qy} \qquad (3.31)$$

where

$$r = p\left[1 - \left(\frac{\omega}{p\,\alpha_L}\right)^2\right]^{1/2}$$
$$q = p\left[1 - \left(\frac{\omega}{p\,\beta_L}\right)^2\right]^{1/2} \qquad (3.32)$$

The stresses and displacements for the case of dry soil can then be written as

$$\tau_{xx} = e^{[i(\omega t-px)]}\{[\lambda(r^2-p^2)-2Gp^2]\left[A_3e^{-ry}+A_4e^{ry}\right] - i(2Gpq)\left[B_1e^{-qy}-B_2e^{qy}\right]\}$$

$$\tau_{yy} = e^{[i(\omega t-px)]}\{[\lambda(r^2-p^2)+2Gr^2]\left[A_3e^{-ry}+A_4e^{ry}\right] + i[2Gpq]\left[B_1e^{-qy}- B_2e^{qy}\right]\} \quad (3.33)$$

$$\tau_{xy} = e^{[i(\omega t-px)]}\{ i(2Gpr)\left[A_3e^{-ry}+ A_4e^{ry}\right] - G(q^2+p^2)\left[B_1e^{-qy}+B_2e^{qy}\right]\}$$

and

$$u_x = e^{[i(\omega t-px)]}\{-ip\left[A_3e^{-ry}+ A_4e^{ry}\right] + q\left[B_1e^{-qy}+ B_2e^{qy}\right]\}$$

$$u_y = e^{[i(\omega t-px)]}\{- r\left[A_3e^{-ry}- A_4e^{ry}\right] - ip\left[B_1e^{-qy}+ B_2e^{qy}\right]\} \quad (3.34)$$

3.3 Coupled Solution

A solution to the free travelling wave problem can now be obtained by combining the solutions for the two zones presented above. These solutions are written in terms of the seven parameters A_1, A_2, and B from the saturated solution and A_3, A_4, B_1 and B_2 from the dry solution. By suitably applying the ground surface and interface boundary conditions, the coupled solution can be generated.

At the free surface, in the dry soil, the vertical stress τ_{yy} and shear stress τ_{xy} are zero. From equations 3.33, two relations can be obtained as:

$$[\lambda(r^2-p^2)+2Gr^2][A_3+A_4] + i[2Gpq][B_1-B_2] = 0 \qquad (3.35)$$

and

$$i[2pr][A_3+A_4] - [q^2+p^2][B_1+B_2] = 0 \qquad (3.36)$$

At the interface between the two zones, the matching conditions are obtained by equating the horizontal and vertical displacements u_x and u_y, as well as the vertical and shear stresses. Equating horizontal displacements at $y = H$, we obtain

$$\begin{aligned} &- ip\,[A_3e^{-rH}+A_4e^{rH}] + q\,[B_1e^{-qH}-B_2e^{qH}] \\ &= - ip\,[A_1e^{\xi_1 H}+\delta_4 A_2 e^{\xi_2 H}] - [\xi_3 B e^{\xi_3 H}] \end{aligned} \qquad (3.37)$$

while equating vertical displacements leads to

$$\begin{aligned} &- r[A_3e^{-rH}-A_4e^{rH}] - ip[B_1e^{-qH}+B_2e^{qH}] \\ &= (\xi_1+\xi_2\delta_4)A_1e^{\xi_1 H} - ip[Be^{\xi_3 H}H] \end{aligned} \qquad (3.38)$$

Equating the total vertical stress at y=H, we obtain

$$\begin{aligned} &(q^2+p^2)[A_3e^{-rH}+A_4e^{rH}] + i(2pq)[B_1e^{-qH}-B_2e^{qH}] \\ &= \left\{\left[2p^2-\left(2+\frac{\lambda^*+\alpha M\delta_1}{G}\right)\Lambda_1^2\right] + \left[2p^2-\left(2+\frac{\lambda^*+\alpha M\delta_2}{G}\right)\Lambda_2^2\right]\right\}[A_1e^{\xi_1 H}] \\ &- i\left\{[2p\xi_3 Be^{\xi_3 H}]\right\} \end{aligned} \qquad (3.39)$$

while equating shear stresses leads to

$$i(2pr)[A_3e^{-rH}-A_4e^{rH}] - (q^2+p^2)[B_1e^{-qH}+B_2e^{qH}]$$
$$= - i2p(\xi_1+\xi_2\delta_4)[A_1e^{\xi_1 H}] - (p^2+\xi_3^2)[Be^{\xi_3 H}] \qquad (3.40)$$

The seventh condition is obtained by setting the pore water pressure equal to zero at the depth H, the location of the GWT. This leads to the relation

$$A_2 = \delta_4 e^{[(\xi_1-\xi_2)H]} \qquad (3.41)$$

where

$$\delta_4 = -\left[\frac{(\alpha+\delta_1)A_1^2}{[(\alpha+\delta_2)A_2^2}\right]$$

These seven conditions are in turn reduceable to a set of six homogeneous algebraic equations which can be placed in matrix form as follows:

$$A_{ij}\,X_j = 0 \qquad i,j = 1 \text{ to } 6 \qquad (3.42)$$

where the nonzero terms are

$A_{11}=[1+(q/p)^2]\exp(rH)$ $A_{12}=2(q/p)\exp(qH)$
$A_{13}=[1+(q/p)^2]\exp(-rH)$ $A_{14}=-2(q/p)\exp(-qH)$
$A_{21}= 2(r/p)\exp(rH)$ $A_{22}=[1+(q/p)^2]\exp(qH)$
$A_{23}=-2(r/p)\exp(-rH)$ $A_{24}=[1+(q/p)^2]\exp(-qH)$
$A_{31}=[1+(q/p)^2]$ $A_{32}=2(q/p)$ $A_{33}=A_{31}$
$A_{34}=-A_{32}$ $A_{41}=-2(r/p)$ $A_{42}=A_{31}$
$A_{43}=2(r/p)$ $A_{44}=A_{33}$ $A_{45}=(2/p)(\xi_1+\xi_2\delta_4)$
$A_{51}=1$ $A_{52}=(q/p)$ $A_{53}=1$
$A_{54}=-(q/p)$ $A_{55}=-(1+\delta_4)$ $A_{61}=(r/p)$
$A_{62}=1$ $A_{63}=-(r/p)$ $A_{64}=1$
$A_{65}=(1/p)(\xi_1+\xi_2\delta_4)$ $A_{66}=-1$

$$A_{35}=\left\{-2(1+\delta_4)+\left[2+\frac{(\lambda^*+\alpha M\delta_1)}{G}\right]\left(\frac{A_1}{p}\right)^2+\left[2+\frac{(\lambda^*+\alpha M\delta_2)}{G}\right]\left(\frac{A_2}{p}\right)^2\right\}$$

For a given set of problem parameters (such as shear modulus, Poisson's ratio, soil density, soil porosity, soil permeability and water compressibility), the solution to equations 3.42 can be obtained for a given frequency, ω, and wave number, p; that is, the value of H which satisfies the six equations can be determined. The specific procedure to obtain this solution is a trial and error process and is still being investigated for typical values of soil parameters. Equations 3.42 can be simplified for the specific case of zero soil permeability, η, that is, assuming that the water is confined to move with the solids. The objective of the numerical procedure is of course to develop information in a form which can indicate how effects of the ground water decrease as the depth, H, increases, such as is shown in Figure 3.2.

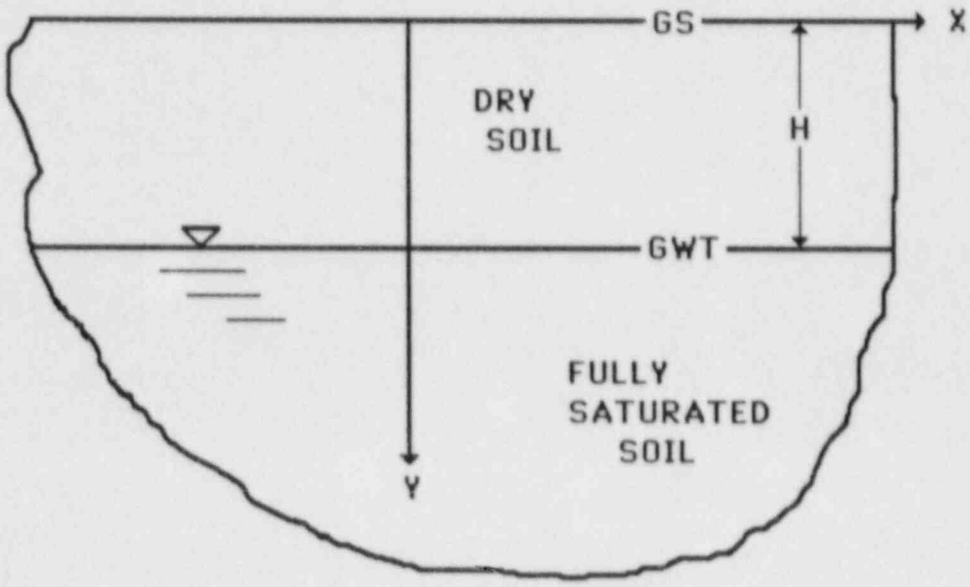

FIGURE 3.1 TWO DIMENSION ELASTIC
PARTIALLY SATURATED HALFSPACE

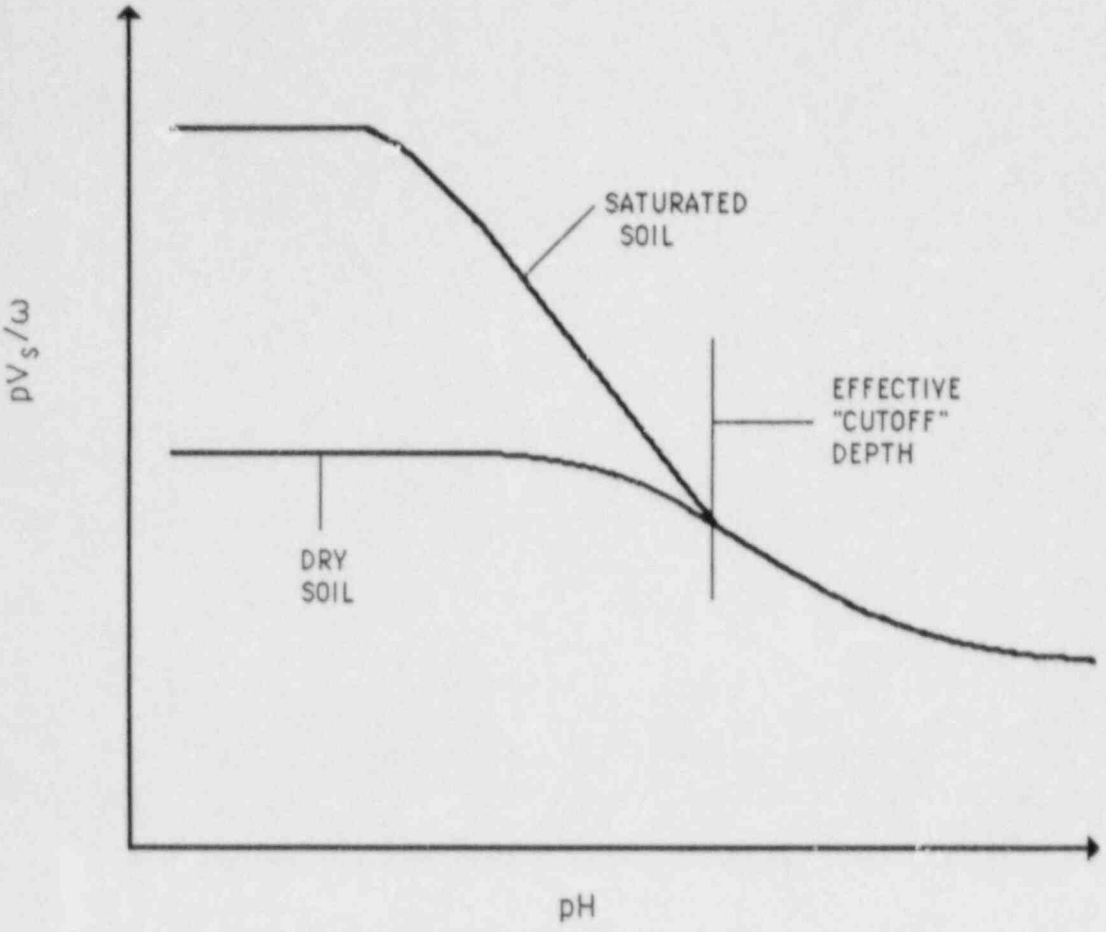

FIGURE 3.2 DETERMINATION OF EFFECTIVE DEPTH FOR GROUND WATER EFFECTS

4.0 FINITE ELEMENT CALCULATIONS

In order to develop solutions for interaction coefficients, a variety of calculations were made using the finite element computer program developed previously (Ref. 1). For the two-phased soil-fluid system, the governing equations of Section 2 were discretized into a set of nodal equations for the displacement parameters (u_x and u_z for the two dimensional problem) and the relative water displacements (w_x and w_z). For any given frequency of steady state motion, the numerical solution is obtained, from which the corresponding soil and water stresses can be calculated.

The specific problem investigated is shown in Figure 4.1. A rigid surface footing of width 2a is located at the surface of the elastic halfspace and moved in the three coordinate directions (horizontal, rocking and vertical modes) in a steady state manner, from which the total forces developed on the footing are calculated. The corresponding influence coefficients are then determined as a function of frequency of the steady state motion. All the data generated is then plotted as a function of dimensionless frequency, which is defined by

$$\lambda = a \Omega / V_s \qquad (4.1)$$

where a is the half footing width, Ω is the input frequency of the steady state motion and V_s is the shear wave velocity of the dry soil. The specific properties of the soil and water used in the calculations are defined in Figure 4.1. These are typical for a relatively stiff silty sand.

As mentioned previously, the primary goal of this numerical study has been to determine the influence of the depth to the ground water table (GWT) on the standard interaction coefficients. In the previous study (Ref. 1), calculations were made for the two cases of either fully saturated soil (GWT at the ground surface) or dry soil (GWT at infinite depth). In this study, the computer program was modified to allow for placing the ground water table at various depths, considering the soil above the GWT as dry. In all the calculations performed, the simplified one-dimensional transmitting boundary originally developed for the previous study was used. As will be seen in some of the following data, this

simplified transmitting formulation is reasonably adequate for these calculations. However, in studying more realistic problems, an improved two dimensional formulation is required. The developments outlined in Section 3 would be would be of significance in such a development. Unfortunately, the scope of this study did not allow for this added development.

Calculations were performed with two meshes for this calculation, the shallower mesh, Model 1, of Figure 4.2 and the deeper mesh, Model 2, shown in Figure 4.3. In both cases, the bottom and side boundaries are subjected to the one-dimensional transmitting boundary condition mentioned above. Obviously, the required symmetry conditions are applied on the left boundary.

4.1 Calculations With Model 1

The first mesh, Model 1, is made up of uniform rectangular elements, fourteen laterally (B/A = 7) and eight vertically (D/A = 4). Based upon previous calcuations, this mesh is adequate to treat wave propagation up to a dimensionless frequency of 2.5 to 3. All calculations presented herein are thus limited to a maximum dimensionless frequency of 2. Calculations were then performed for a variety of configurations, moving the GWT from the ground surface to a depth specified by H/A = 3.5 (seven elements below the footing. Figure 4.4 presents horizontal interaction coefficients (stiffness and damping) for a variety of the depth to the GWT. As may be noted from the lower figure, the damping coefficient rapidly decays from the fully saturated case to the dry case, until at a depth ratio of 1.0, the damping coefficients are essentially identical to the dry problem. From the upper plot of Figure 4.4, however, it may be noted that the horizontal stiffness coefficient does not as quickly converge to the dry case. Similar data is shown in Figure 4.5, which shows additional results for the lower depths to the GWT. As can be seen, the damping coefficients still show the independence with the GWT at these depths, with the stiffness coefficients essentially showing relatively uniform results below a dimensionless depth of 2.0.

Similar data from Model 1 for the rocking stiffness and damping in Figure 4.6 and 4.7. As may be noted, the damping essentially approaches the dry data at depths below 0.5 while the rocking stiffness converges to the dry case at depths

of 1.5. The small differences at the higher frequencies probably are unreal if actual material damping effects were considered in the calculations. All the data at the deeper depths shown in Figure 4.7 show essentially complete agreement with the dry data at depths below 1.5.

Unfortunately, no similar simple conclusions can be developed for the vertical interaction coefficient, the results for which are shown in Figures 4.8 and 4.9 for the various depths to the GWT. At low values of dimensionless frequency, below a value of about 0.8, the damping coefficients are reasonably close to the fully dry case. At higher frequencies, however, the damping coefficients are significantly different from the dry data. A possible explanation can be the following. At shallower depths to the GWT, the damping coefficient is higher than the dry case, indicating that the energy loss through the water-soil coupling (through soil permeability effects) is important since soil/water relative motions are larger. At the lower depths to the GWT, however, the water interface may prevent radiation energy loss usually associated with the dry halfspace. But at the same time, energy loss due to permeability may be small since the relative motions between water and soil at these depths are small. In any case, the energy loss associated with this vertical motion is composed of two parts, one due to relative soil/water movements and the second due to radiation effects. The specific amount of each is apparently frequency as well as depth dependent.

4.2 Calculations With Model 2

As noted from Figure 4.3, the mesh of Model 2 extends to a depth fifty percent deeper than that of Model 1, with the same side boundary location. Again, one dimensional transmitting boundary conditions were applied at the bottom and side boundaries. The primary goal of these calculations was to see if the vertical coefficients settle down to the dry data at these deeper depths. First, however, a comparison between the meshes was investigated to see if the transmitting boundary is adequate enough to compare these data between the two meshes. The horizontal interaction coefficents are shown in Figure 4.10 for the two cases, both with the GWT at a depth of 3.5A. Both the damping and stiffness coefficients are adequately replicated by this boundary, with the differences in the stiffness coefficients associated with a gross frequency of the mesh.

The comparison of the rocking data is presented in Figure 4.11. As may be noted, at the higher frequencies of interest, the results are good. However, below the dimensionless frequency of about 0.8, the boundary effects appear to be important. The damping data is reasonably good over the entire frequency range of interest. Both of the vertical interaction coefficients show excellent agreement over the entire frequecy range of interest, as seen in Figure 4.12. This indicates that under a vertical load, the bottom boundary primary moves in a one-dimensional mode and the one-dimensional formulation is reasonable. Since the vertical problem is the primary purpose of the extended calculations, it is felt that comparisons for the deeper depths to the GWT are adequate for these purposes. However, as mentioned previously, the improved two dimensional soil/water transmitting boundary formulation is required for specific response calculations.

A comparison of the deeper results is shown in Figure 4.13 for the horizontal interaction coefficients. Since it was already concluded that below a depth of about 1.5, the influence of the GWT are small for this problem. The differences that may be noted between the dry case and the results from Model 2 can be ascribed entirely to the boundary effects as discussed previously, since the results for the dry case were developed with Model 1. A similar conclusion can be reached for the rocking data, shown in Figure 4.14. Again the differences at the low frequency is due to boundary effects.

The vertical data, which shows little impact of the bottom boundary formulation, is presented in Figure 4.15. As can be noted, the stiffness data shows good correlation at depths below a value of about three. The damping data, although showing reasonable correlation at these depths, still shows indications of differences at the higher frequencies of interest, as previously discussed.

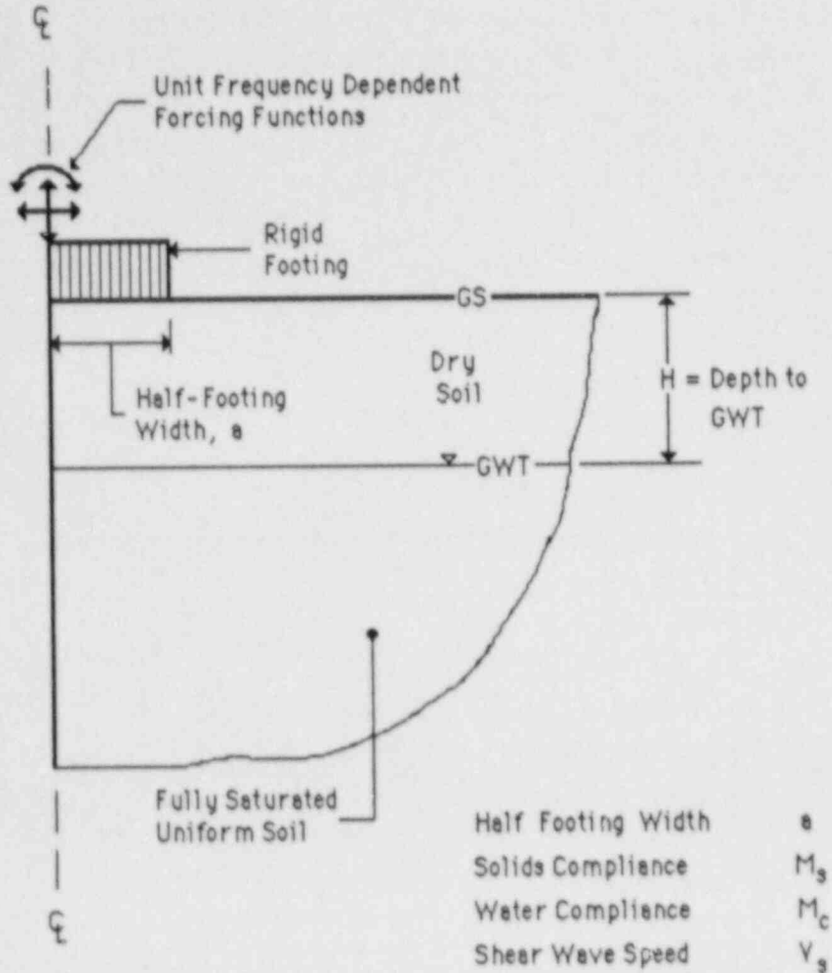

Half Footing Width	a	300 inches
Solids Compliance	M_s	14,000 psi
Water Compliance	M_c	293,900 psi
Shear Wave Speed	V_s	448.72 fps
Dry P Wave Speed	V_c	777.19 fps
Poisson's Ratio	ν	0.25
Dry Soil Density	γ_d	107.47 pcf
Sat. Soil Density	γ_s	129.31 pcf
Soil Permeability	k	10^{-1} to 10^{-6} cm/sec

FIGURE 4.1 RIGID FOOTING ATOP AN ELASTIC SOIL IN A TWO DIMENSIONAL PLANE STRAIN CONFIGURATION

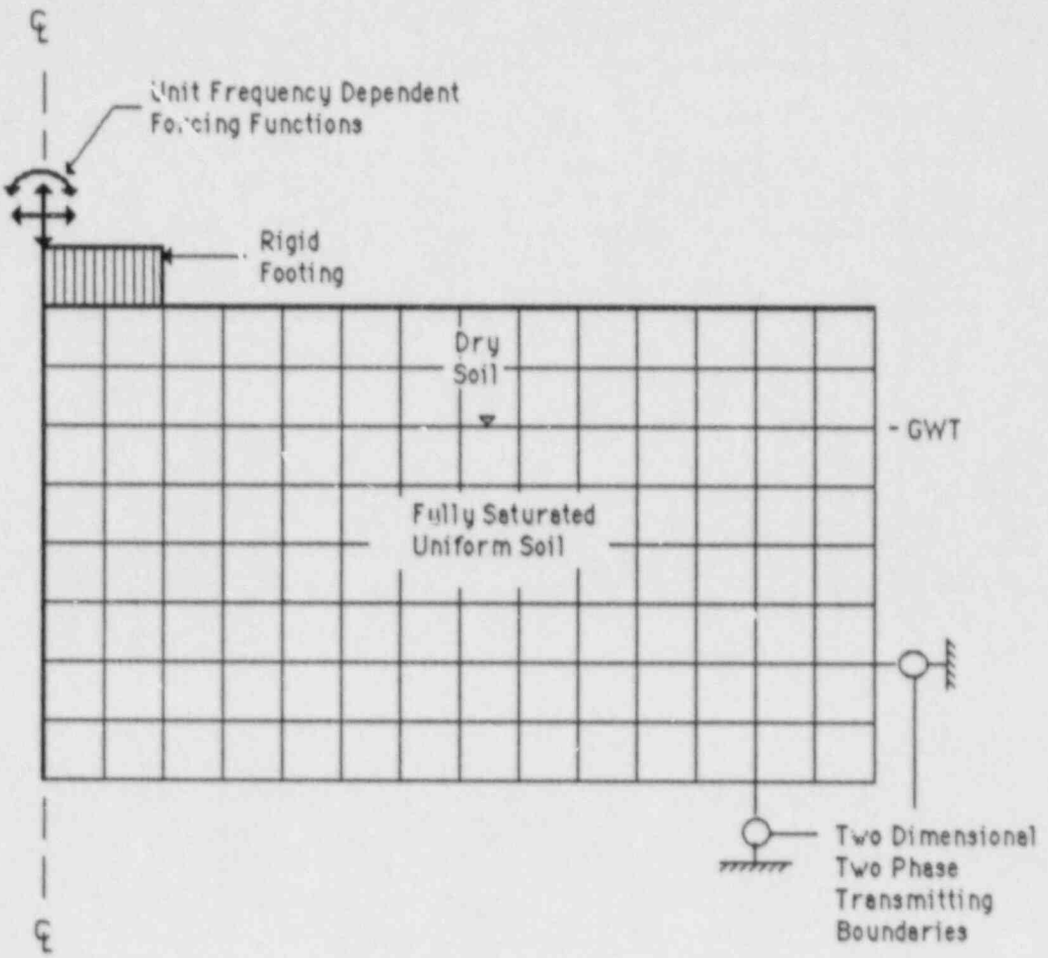

FIGURE 4.2 MODEL 1 FINITE ELEMENT MESH

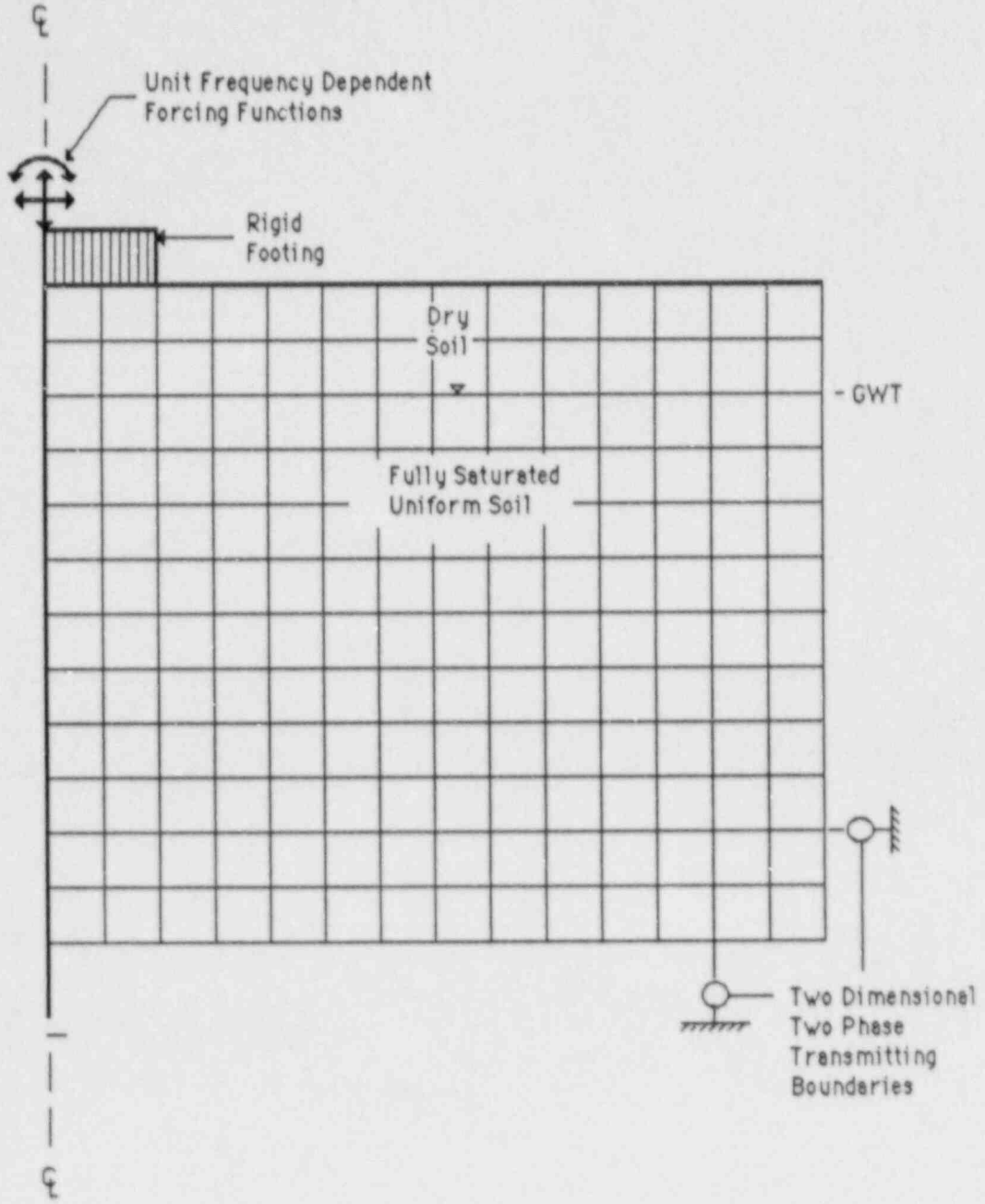

FIGURE 4.3 MODEL 2 FINITE ELEMENT MESH

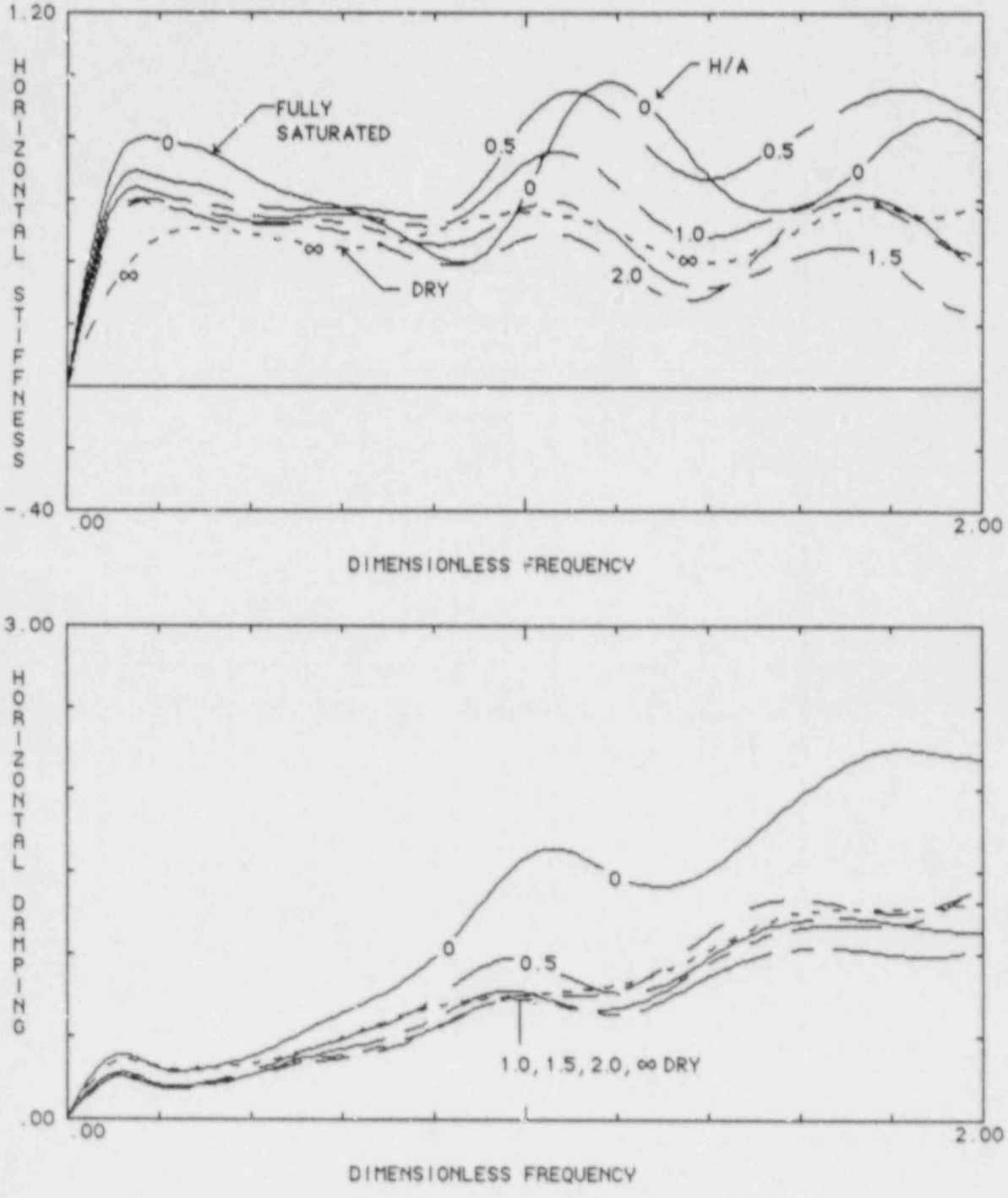

FIGURE 4.4 HORIZONTAL INTERACTION COEFFICIENTS USING MODEL 1 FOR A UNIFORM SOIL

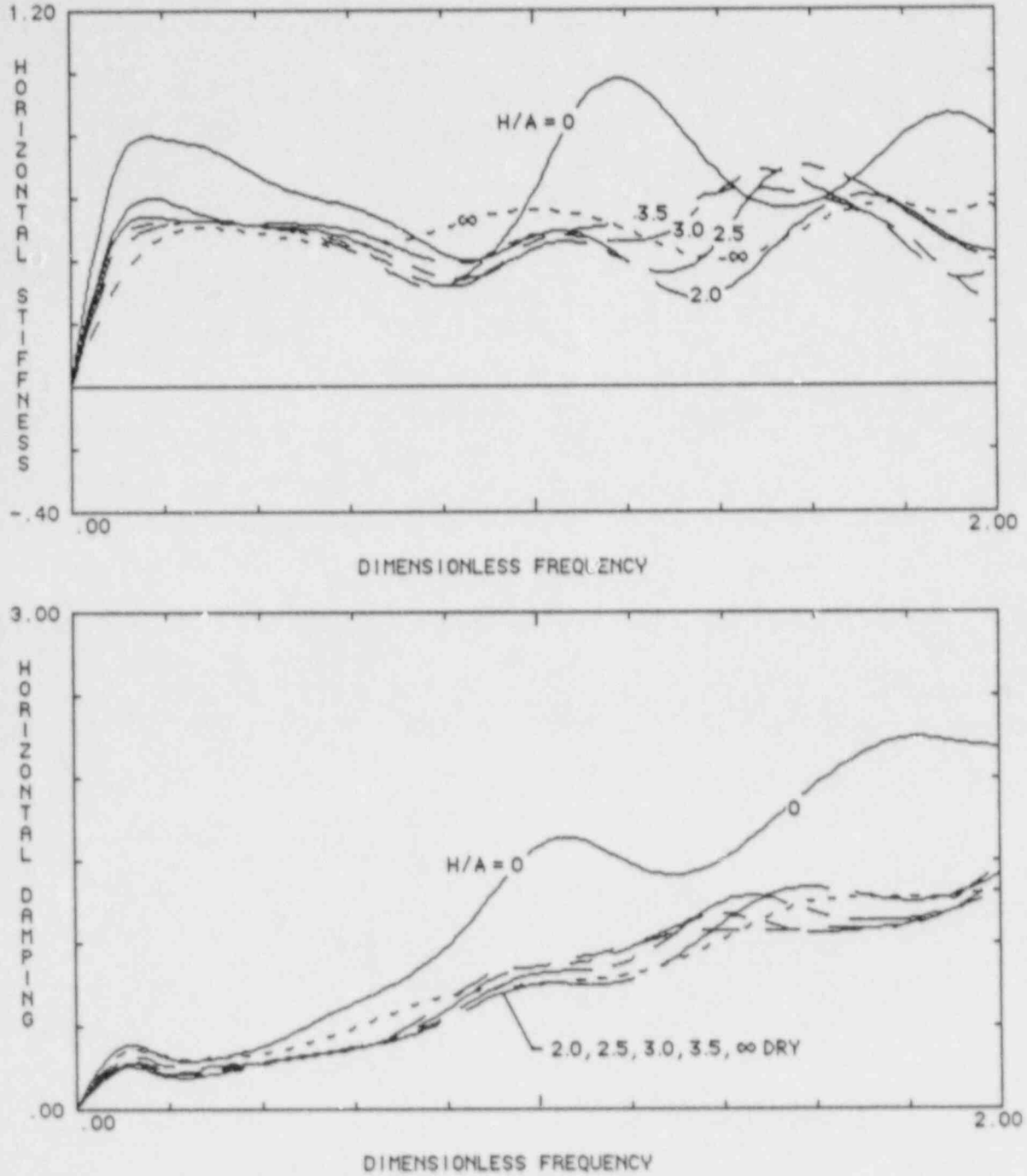

FIGURE 4.5 HORIZONTAL INTERACTION COEFFICIENTS USING MODEL 1 FOR A UNIFORM SOIL

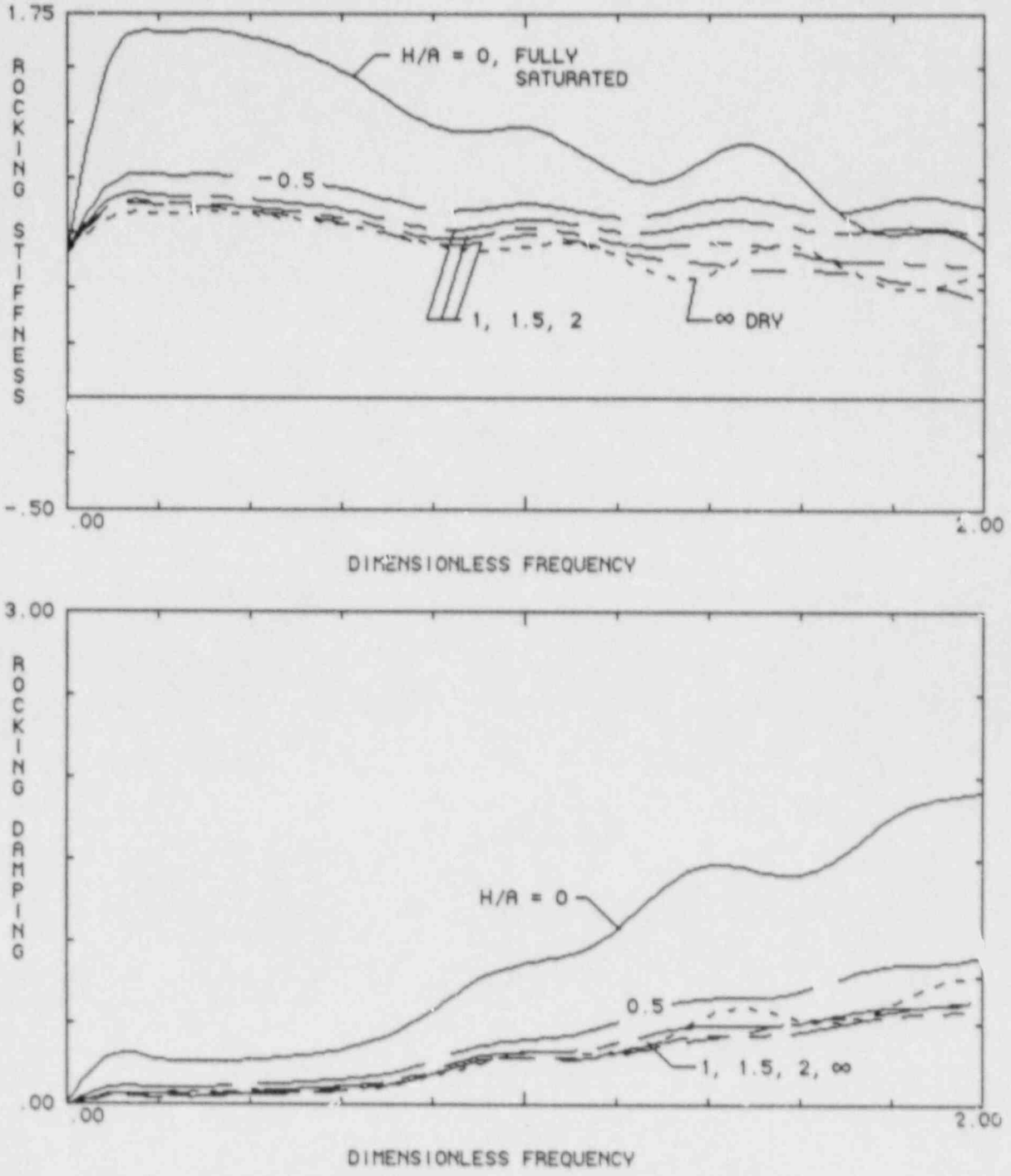

FIGURE 4.6 ROCKING INTERACTION COEFFICIENTS USING MODEL 1 FOR A UNIFORM SOIL

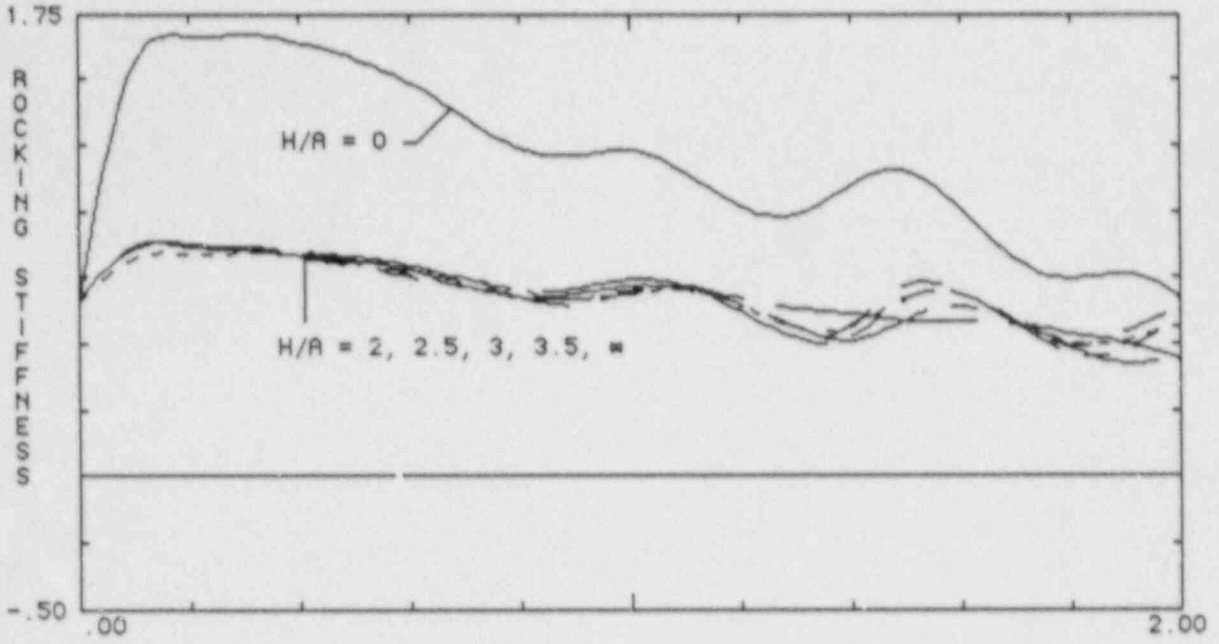

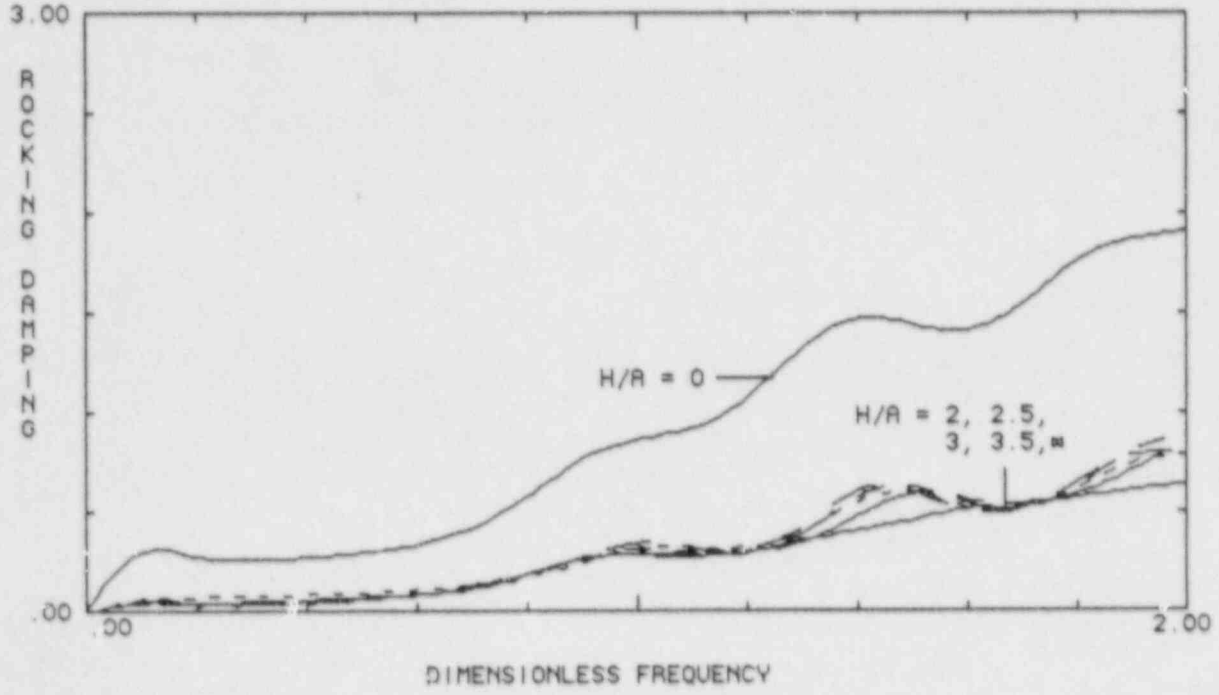

FIGURE 4.7 ROCKING INTERACTION COEFFICIENTS USING MODEL 1 FOR A UNIFORM SOIL

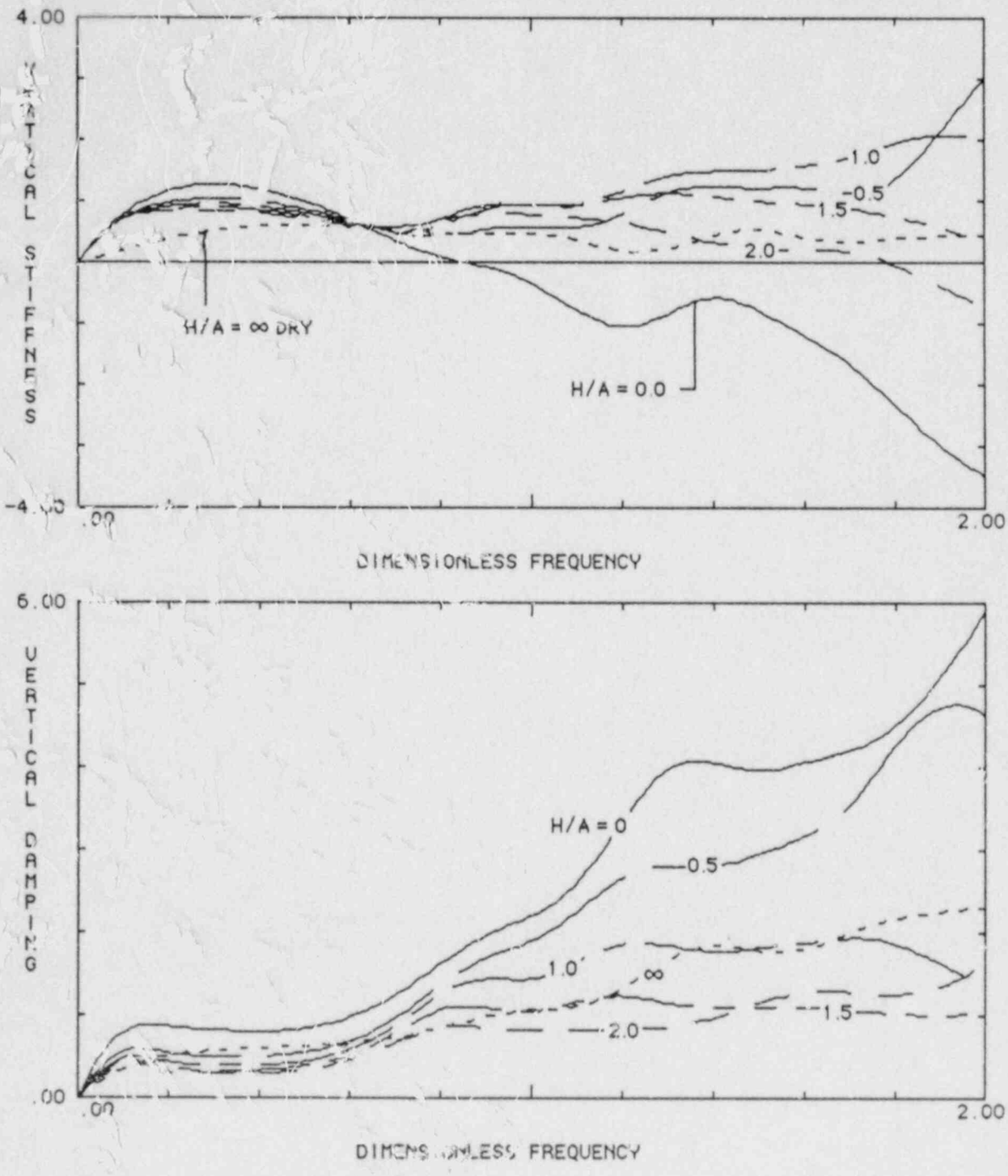

FIGURE 4.8 VERTICAL INTERACTION COEFFICIENTS USING MODEL 1 FOR A UNIFORM SOIL.

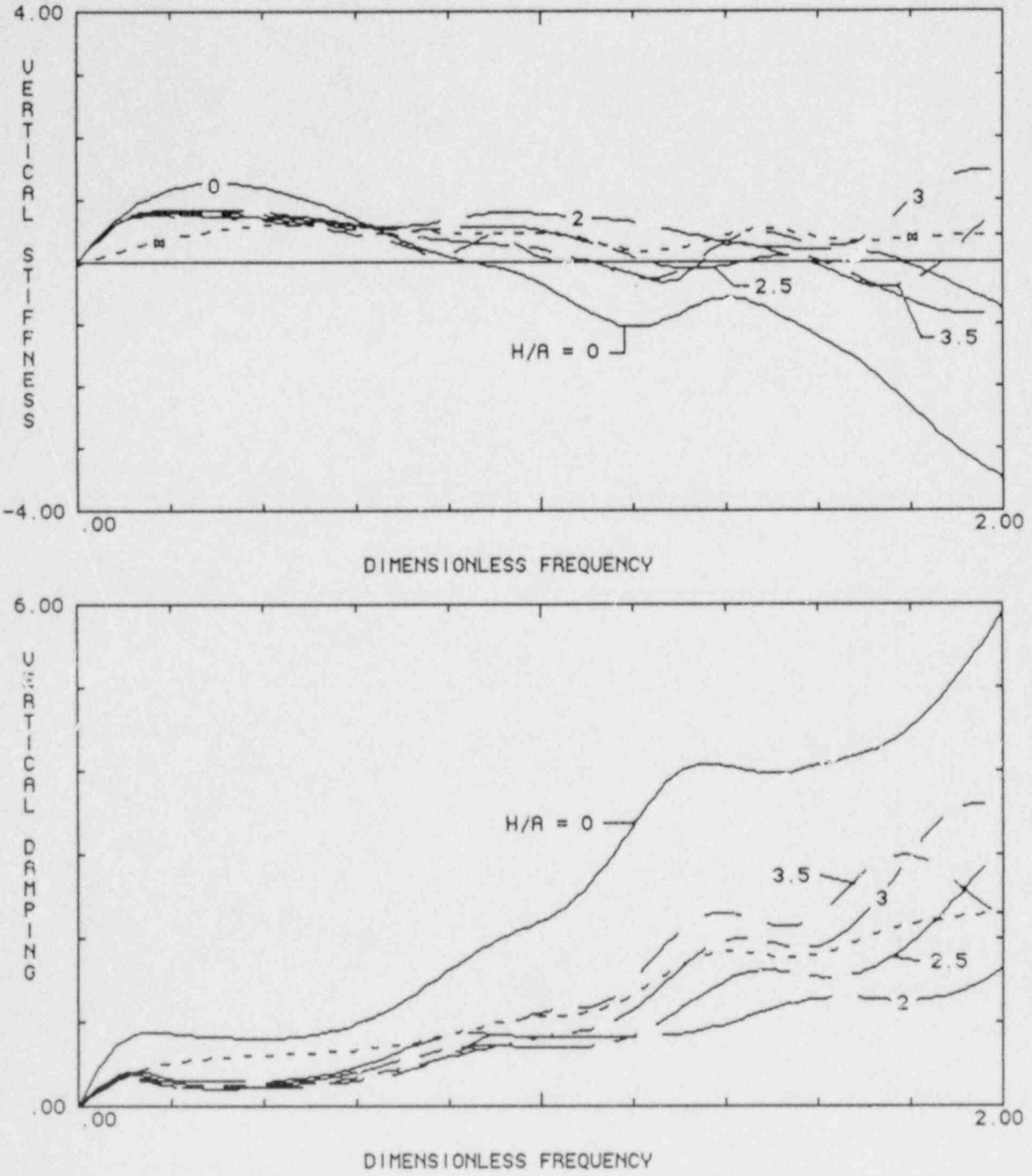

FIGURE 4.9 VERTICAL INTERACTION COEFFICIENTS USING MODEL 1 FOR A UNIFORM SOIL

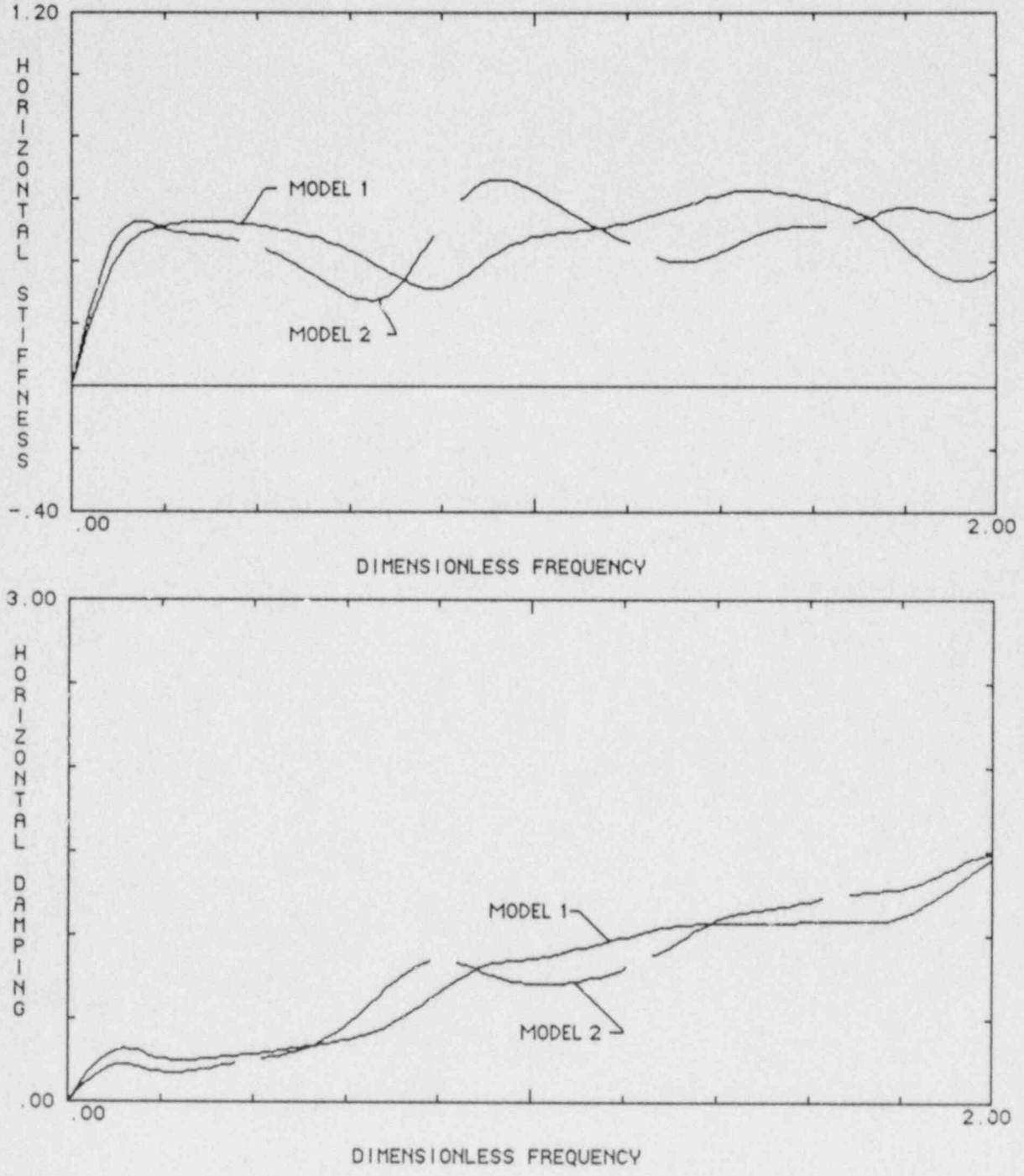

FIGURE 4.10 COMPARISON OF HORIZONTAL INTERACTION COEFFICIENTS FOR TWO MESHES

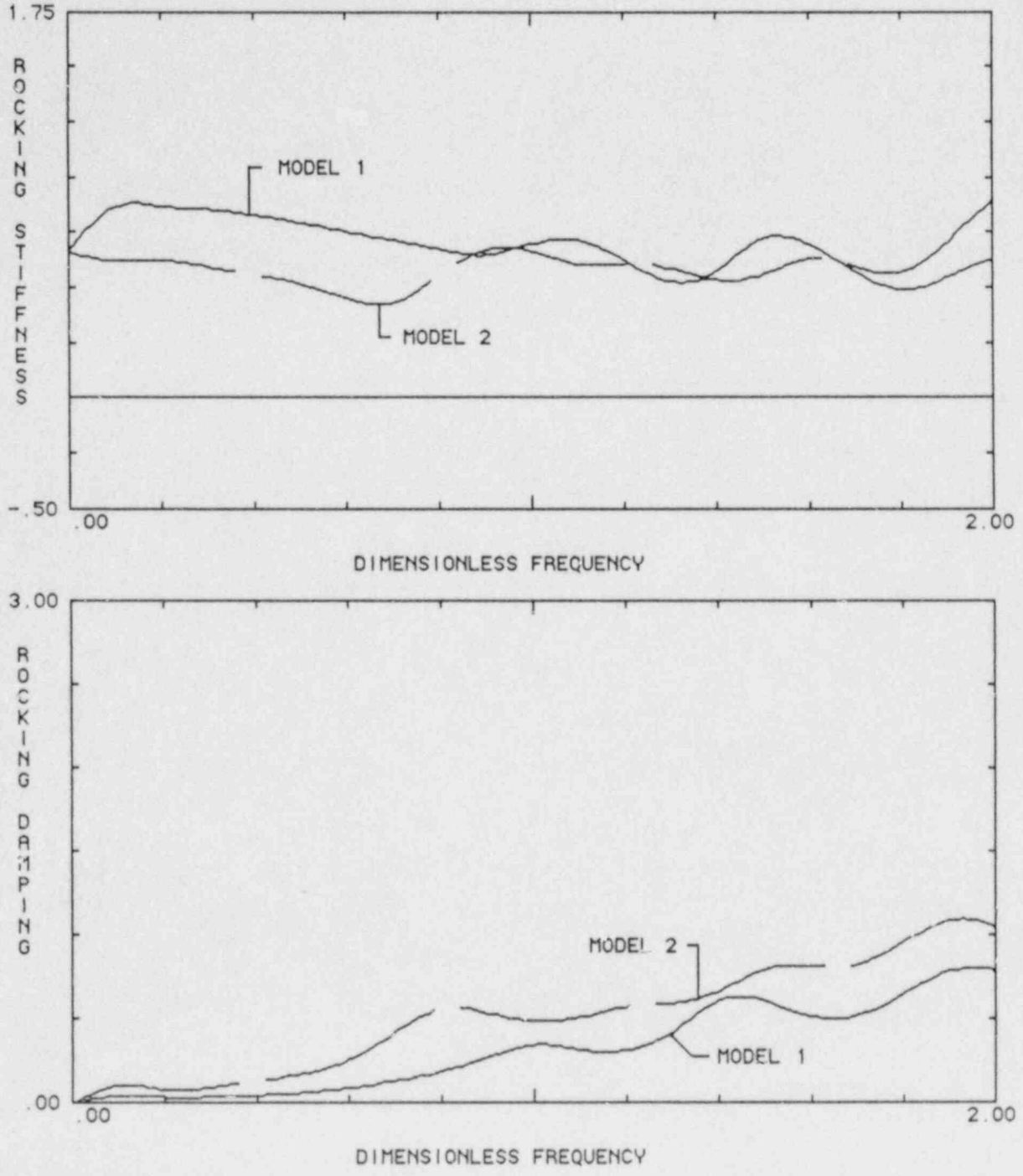

FIGURE 4.11 COMPARISON OF ROCKING INTERACTION COEFFICIENTS FOR TWO MESHES

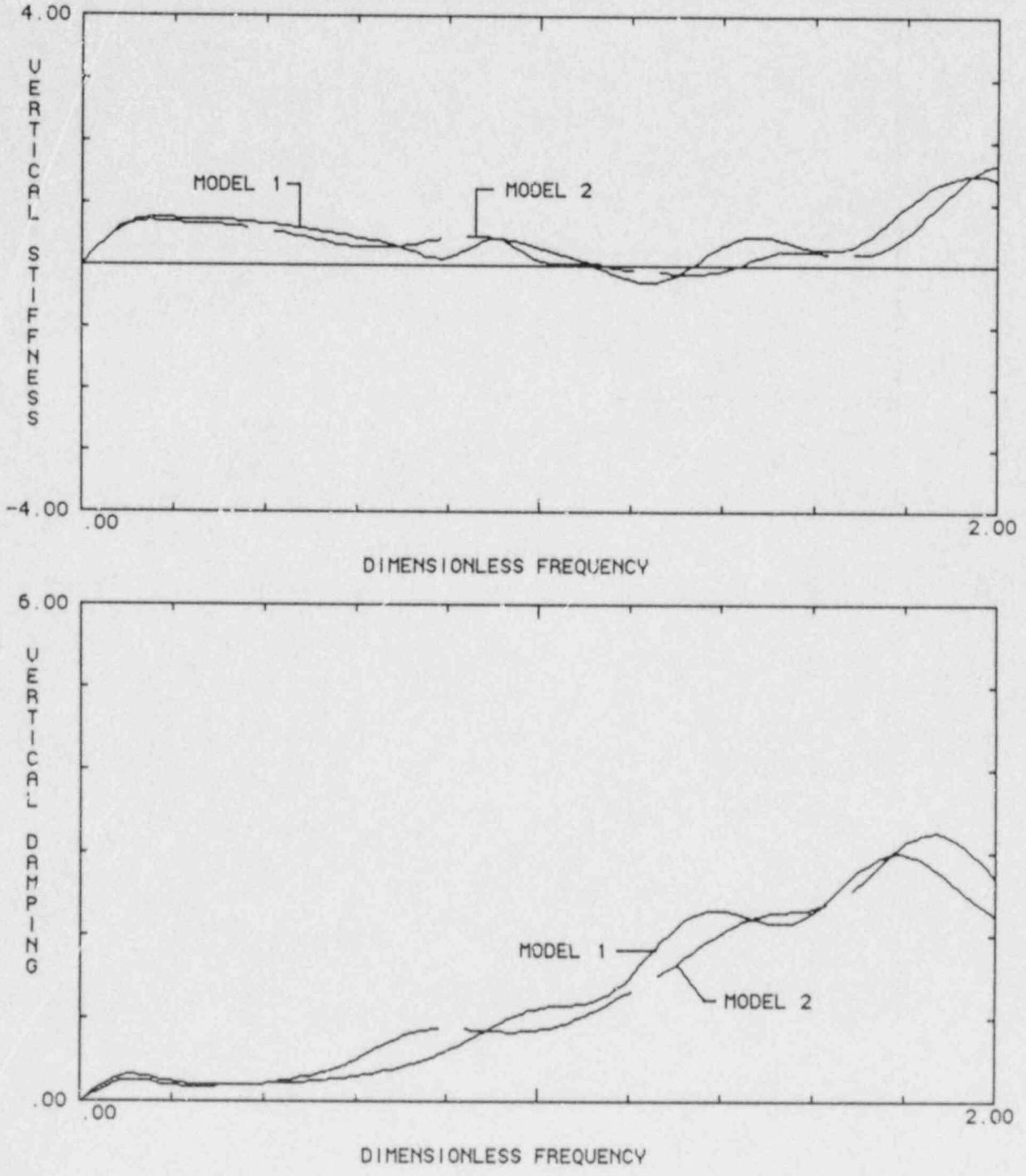

FIGURE 4.12 COMPARISON OF VERTICAL INTERACTION COEFFICIENTS FOR TWO MESHES

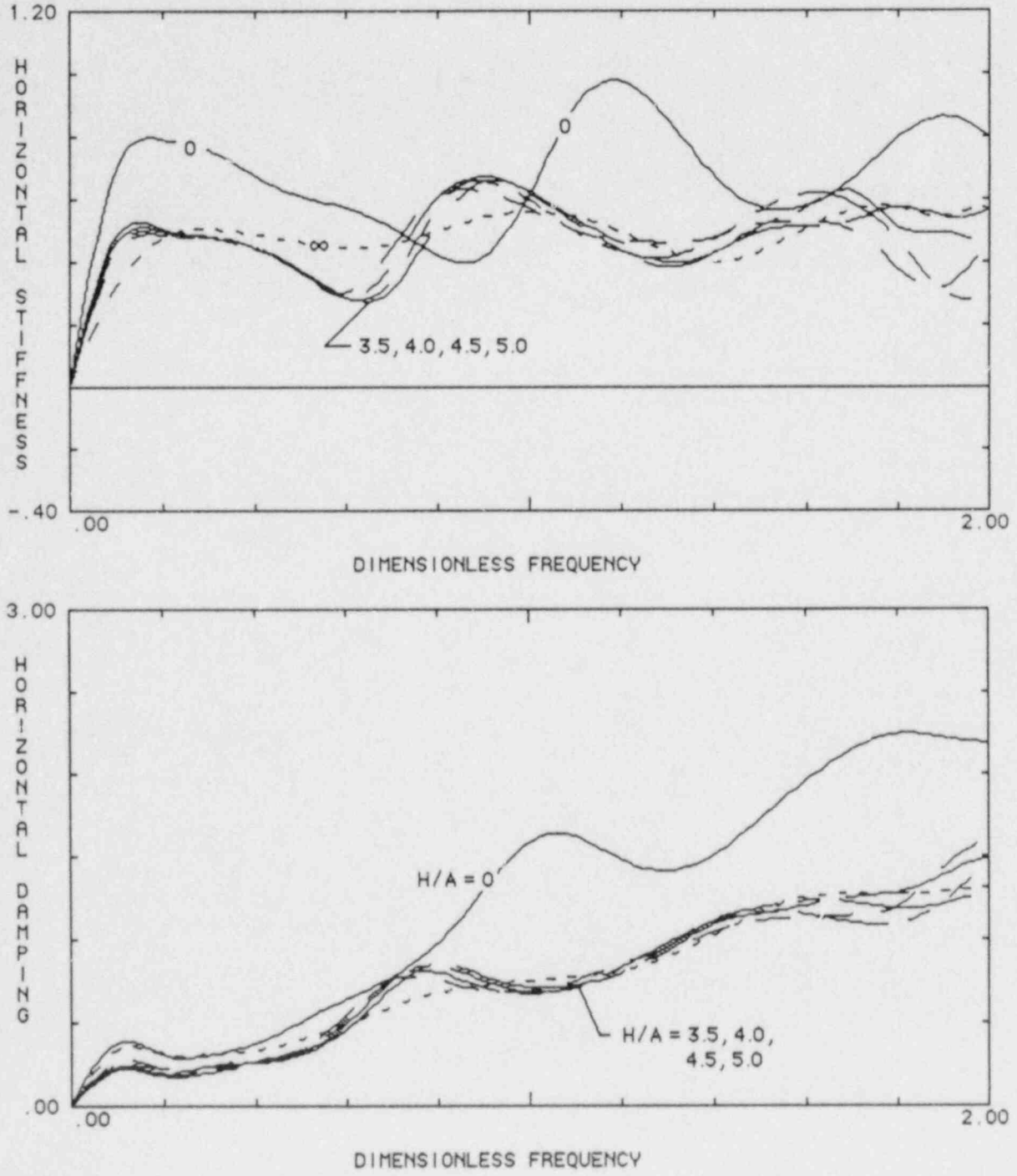

FIGURE 4.13 HORIZONTAL INTERACTION COEFFICIENTS FROM MODEL 2

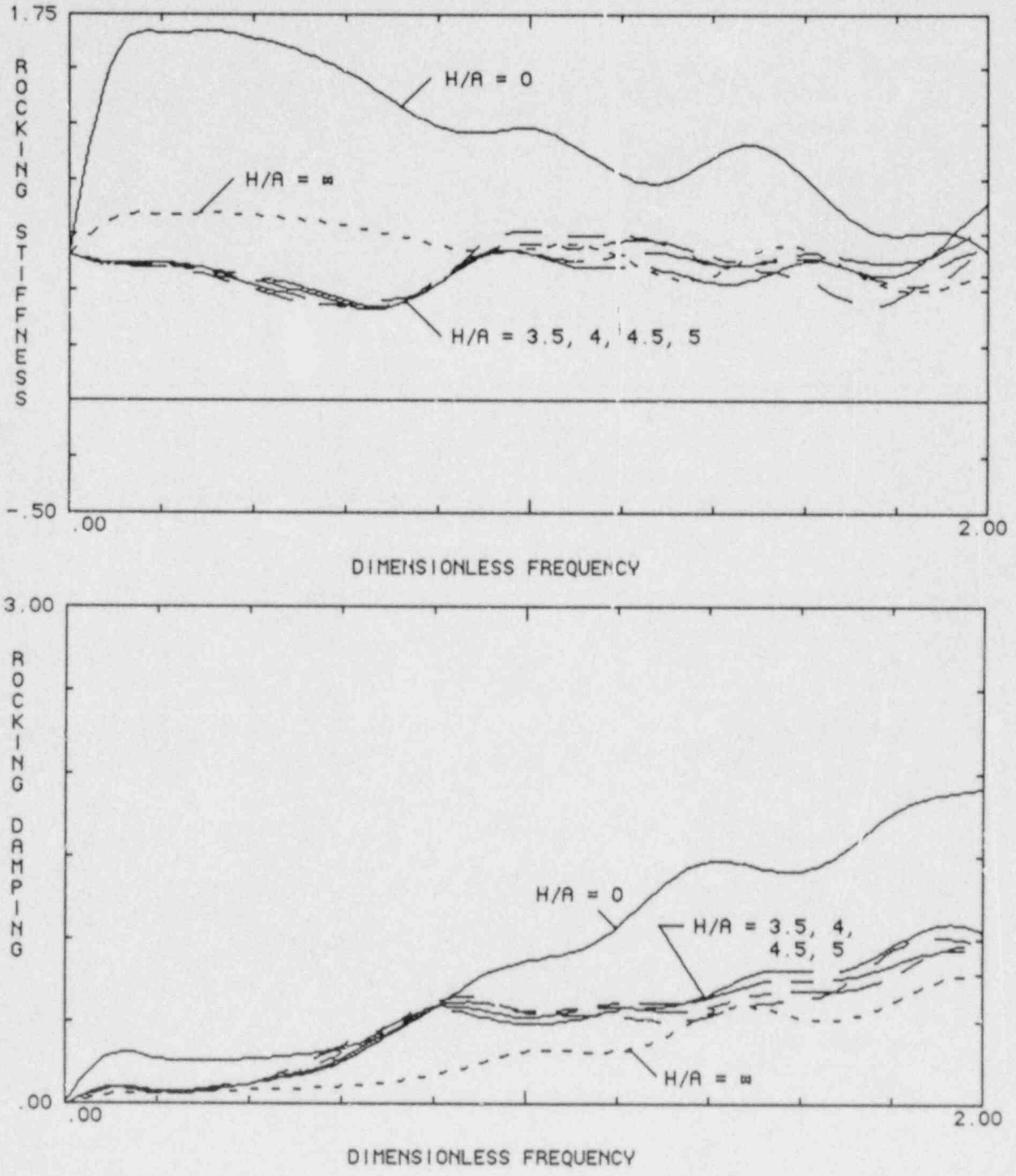

FIGURE 4.14 ROCKING INTERACTION COEFFICIENTS FROM MODEL 2

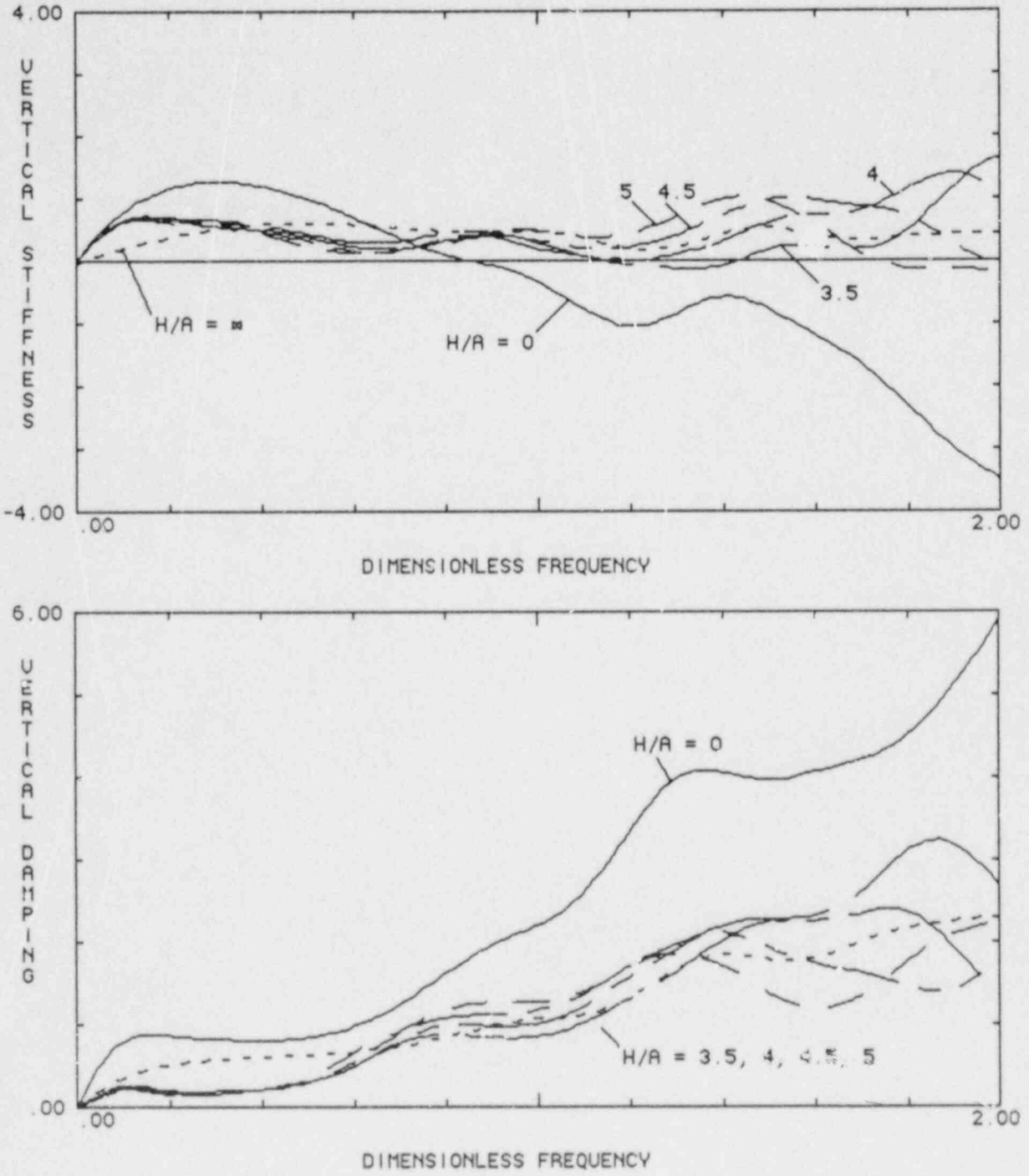

FIGURE 4.15 VERTICAL INTERACTION COEFFICIENTS FROM MODEL 2

5.0 CONCLUSIONS AND RECOMMENDATIONS

The results of this study indicate that pore water effects can play a significant role in the soil-structure interaction process. Based upon the calculations presented in Section 4, the following conclusions can be drawn. First, if the ground water table is located at the depth of the foundation, the pore water causes the horizontal interaction coefficients (both stiffness and damping) to increase by more than 50%. As the GWT moves away from the foundation, this effect decreases. At a depth ratio of 1.0 (depth from the foundation to half width of foundation), the damping coefficient approaches the dry case while stiffness coefficient reaches the dry case values at a depth ratio of about 2.0. Similar results for the rocking case indicate that the damping coefficient approaches the dry value very rapidly, at a depth ratio of 0.5, while the corresponding stiffness coefficient converges at a depth ratio of 1.5.

For the vertical mode of response, the results are not so clear and can be considered as frequency dependent. Based upon the results generated to date, it appears that below a depth ratio of about 3.0, the stiffness coefficients seem to converge to the dry data. However, the damping data, contrary to the behavior noted for the other coefficients, does not seem to converge to the dry solution, but rather to oscillate about it. This may be due to the effect of the GWT in preventing radiation effects away from the foundation. At the lower frequency range (dimensionless frequencies less than about 1.5) the damping appears to be similar to the dry case. At the higher frequencies, however, the results are not as conclusive.

As recommended in the previous study (Ref. 15), it is suggested that future work concentrate on the development of a two dimensional transmitting boundary formulation. The results developed herein indicate that the simpler one dimensional approach, although adequate to investigate general trends in the computations, is not adequate enough for the detailed capabilities required in calculations associated with an actual facility. It is recommended that the approach follow the developments presented in Section 3 of this report. With the solutions which can be developed from these calculations, the formulation will be relatively straight forward. The computer results will be significantly enhanced with this major improvement. With this improved formulation, further numerical results can be generated to assess the impact of pore water on the

interaction process.

An area of important consideration is to use the results of these linear calculations to investigate the potential impact of soil liquefaction on structural response. Even though the liquefaction problem is a highly nonlinear process, the results of the linear calculations can be used to estimate where under a given foundation the pore water effects can be important. This data, combined with the more empirical data available for liquefaction based on soil type, such as that presented in Refs. 36 and 37, can be used to judge if and when liquefaction can be an important issue.

6.0 REFERENCES/BIBLIOGRAPHY

1. J.L. Auriault, L. Borne and R. Chambon, "Dynamics of Porous Saturated Media; Checking of the Generalized Law of Darcy", Journal of Acoustical Society of America, vol. 77 (5), May 1985

2. P. Bettess and O.C. Zienkiewicz, "Diffraction and Refraction of Surface Waves Using Finite and Infinite Elements", Inter. Journal for Numerical Methods in Engineering, vol 11, 1977

3. M.A. Biot, "General Theory of Three Dimensional Consolidation", Journal of Applied Physics, vol 12, Febr. 1941

4. M.A. Biot, "Consolidation Settlement Under a Rectangular Load Distribution", Journal of Applied Physics, vol 12, May 1941

5. M.A. Biot, "Consolidation Settlement of a Soil with an Impervious Top Surface", Journal of Applied Physics, vol 12, July, 1941

6. M.A. Biot, "Theory of Elasticity and Consolidation for a Porous Anisotropic Solid", Journal of Applied Physics, vol 26 (2), Febr. 1955

7. M.A. Biot and D.G.Willis, "The Elastic Coefficients of the Theory of Consolidation", Journal of Applied Mechanics, vol 24, Dec. 1957

8. M.A. Biot, "Theory of Propagation of Elastic Waves in a Fluid-Saturayed Porous Solid. I. Low-Frequency Range", Journal of the Acoustical Society of America, vol 28 (2), Mar. 1956

9. M.A. Biot, "Mechanics of Deformation and Acoustic Propagation in Porous Media", Journal of Applied Physics, vol 33 (4), Apr. 1962

10. Y.K. Cheung and T.P. Khatua, " A Finite Element Solution Program for Large Structures", Inter. Journal for Numerical Methods in Engineering, vol 10,, 1976, pp 401-412

11. C.J. Costantino, "Finite Element Approach to Stress Wave Problems", Journal of the Engineering Mechanics Division, ASCE, June, 1966

12. C.J. Costantino, "Two-Dimensional Wave Propagation Through Nonlinear Media", Journal of Computational Physics, vol 4 (2), Aug. 1969

13. C.J. Costantino, L.A. Lufrano and C.A. Miller, "Mesh Size Criteria for Soil Amplification Studies", Proceedings, 3rd Inter. Conference on Structural Mechanics in Reactor Technology, London, Sept. 1975

14. C.J. Costantino, C.A. Miller and L.A. Lufrano, "Soil-Structure Interaction Parameters from Finite Element Analyses", Proceedings, Conference on Extreme Load Conditions, Berlin, Sept. 1975

15. C. J. Costantino, "Soil-Structure Interaction, Volume 3, Influence of Ground Water", NUREG/CR-4588, BNL-NUREG-51983, April, 1986

16. J. Ghaboussi and E.L. Wilson, "Variational Formulation of Dynamics of Fluid-Saturated Porous Elastic Solids", Journal of Engineering Mechanics Division, ASCE, vol 98 (EM4), Aug. 1972

17. J.A. Gutierrez, "A Substructure Method for Earthquake Analysis of Structure-Soil Interaction", Earthquake Engineering Research Center, Report No. 76-9, Apr. 1976

18. R.H. Lung, "Seismic Analysis of Structures Embedded in Saturated Soils", Ph.D Dissertation, Department of Civil Engineering, City University of New York, 1980

19. J. Lysmer and R.L. Kuhlemeyer, "Finite Dynamic Model for Infinite Media", Journal of Engineering Mechaincs Division, ASCE, vol 95 (EM4), Aug. 1969

20. C.C. Mei and M.A. Foda, "Wave Induced Responses in a Fluid Filled Poroelastic Solid with a Free Surface - a Boundary Layer Theory", Geophysics Journal of the Royal Astronomical Society, vol. 66 (3), 1981

21. C.C. Mei and A.E. Mynett, "Earthquake Induced Stresses in a Poroelastic Foundation Supporting a Rigid Structure", Geotechnique, vol. 33 (3), 1983

22. C.C. Mei, I.S. Boon and Y.S. Chen, "Dynamic Response in a Poroelastic Ground Induced by a Moving Air Pressure", Wave Motion, Elsevier Science Publishers, 1985

23. P.R. Ogushwitz, "Applicability of the Biot Theory; Low-Porosity Materials", Journal of Acoustical Society of America, vol. 77 (2), Feb. 1985

24. J.H. Prevost, "Mathematical Modeling of Monotonic and Cyclic Undrained Clay Behavior", Inter. Journal of Numerical and Analytical Methods in Geomechanics, vol 1 (2), 1977

25. J.H. Prevost, "Anisotropic Undrained Stress-Strain Behavior of Clays", Journal of Geotechnical Engineering Division, ASCE, vol 104 (GT8), Aug. 1978

26. J.H. Prevost, "Mechanics of Continuous Porous Media", International Journal of Engineering Science, 1980

27. J.H. Prevost, "Non-Linear Transient Phenomena in Soil Media", Mechanics of Engineering Materials, ed. C.S. Desai and R.H. Galagher, John Wiley & Sons 1984

28. J.M. Roesset and M.M. Ettouney, "Transmitting Boundaries: A Comparison", Inter. Journal for Numerical and Analytical Methods in Geomechanics, vol 1, 1977

29. R.D. Stoll, "Acoustic Waves in Ocean Sediments", Geophysics, vol. 42 (4), June 1977

30. R.D. Stoll, "Experimental Studies of Attenuation in Sediments", Journal of Acoustical Society of America, vol 66 (4), Oct. 1979

31. R.D. Stoll, "Theoretical Aspects of Sound Transmission in Sediments", Journal of Acoustical Society of America, vol 68 (5), Nov. 1980

32. R.D. Stoll, "Reflection of Acoustic Waves at a Water-Sediment Interface", Journal of Acoustical Society of America, vol 70 (1), July 1981

33. R.D. Stoll and G.M. Bryan, "Wave Attenuation in Saturated Sediments", Journal of the Acoustical Society of America, vol 47 (5), 1970

34. R.S. Sandhu and K.S. Pister, "A Variational Principle for Linear Coupled Field Problems in Continuum Mechanics", Inter. Journal of Engineering Science, vol 8, 1970, pp 989-999

35. R.S. Sandhu and E.L. Wilson, "Finite Element Analysis of Seepage in Elastic Media", Journal of Engineering Mechanics Division, ASCE, vol 95 (EM3), June 1969

36. M.M. Zaman and G.C. Biswas, "Effects of Soil Liquefaction on Seismic Response of Nuclear Power Plants", Proceedings, 8th Inter. Conference on Structural Mechanics in Reactor Technology, Brusselss, Belgium, Aug. 1985

37. O.C. Zienkiewicz, C.T. Chang and E. Hinton, "Nonlinear Seismic Response and Liquefaction", Inter. Journal for Numerical and Analytical Methods in Geomechanics, vol. 2, 1978, pp 381-404

38. O.C. Zienkiewicz and T. Shiomi, "Dynamic Behavior of Saturated Porous Media: The Generalized Biot Formulation and Its Numerical Solution", Imter. Journal for Numerical and Analytic Methods in Geomechanics, vol. 8, 1984, pp 71-96

NRC FORM 335 (2-84) NRCM 1102, 3201, 3202

U.S. NUCLEAR REGULATORY COMMISSION

BIBLIOGRAPHIC DATA SHEET

SEE INSTRUCTIONS ON THE REVERSE

1. REPORT NUMBER (Assigned by TIDC and Vol. No., if any)

BNL-NUREG-52039

NUREG/CR-4784

2. TITLE AND SUBTITLE

"Influence of Ground Water on Soil-Structure Interaction"

3. LEAVE BLANK

4. DATE REPORT COMPLETED

MONTH: October YEAR: 1987

5. AUTHOR(S)

C.J. Costantino

A.J. Philippacopoulos

6. DATE REPORT ISSUED

MONTH YEAR

7. PERFORMING ORGANIZATION NAME AND MAILING ADDRESS (Include Zip Code)

Dept. of Nuclear Energy
Brookhaven National Laboratory
Upton, NY 11973

8. PROJECT/TASK/WORK UNIT NUMBER

9. FIN OR GRANT NUMBER

A-3242

10. SPONSORING ORGANIZATION NAME AND MAILING ADDRESS (Include Zip Code)

Office of Nuclear Regulatory Research
U.S. Nuclear Regulatory Commission
Washington, D.C. 20555

11a. TYPE OF REPORT

formal

b. PERIOD COVERED (Inclusive dates)

12. SUPPLEMENTARY NOTES

13. ABSTRACT (200 words or less)

This report presents a summary of the second year's effort on the subject of the influence of foundation ground water on the SSI phenomenon. A finite element computer program, developed during the first year's effort, was used to study the impact of depth to the ground water surface on the SSI problem. The formulation used therein is based on the Biot dynamic equations of motion for both the solid and fluid phases of a typical soil. Frequency dependent interaction coefficients were then generated for the two-dimensional plane problem of a rigid surface footing moving against a linear soil. The soil is considered dry above the GWT and fully saturated below. The results indicate that interaction coefficients are significantly modified as compared to the comparable values for a dry soil, particularly for the rocking mode of response, if the GWT is close to the foundation. As the GWT moves away from the foundation, these effects decrease in a relatively orderly fashion for both the horizontal and rocking modes of response. For the vertical interaction coefficients, the rate of convergence to the dry solution is frequency dependent.

Calculations were made to study the impact of the modified interaction coefficients on the response of a typical nuclear reaction building. The amplification factors for a stick model placed atop a dry and saturated soil were computed. It was found that pore water caused the rocking response to decrease and translational response to increase over the frequency range of interest, as compared to the response on dry soil.

14. DOCUMENT ANALYSIS - a. KEYWORDS/DESCRIPTORS

saturated soils, foundations, pore water, impedances, interaction, parameters

b. IDENTIFIERS/OPEN-ENDED TERMS

15. AVAILABILITY STATEMENT

Unlimited

16. SECURITY CLASSIFICATION

(This page) Unclassified

(This report) Unclassified

17. NUMBER OF PAGES

18. PRICE